suggesting that modification of mutant AR differs in the nucleus and cytoplasm. We also need to further clarify which degradation process affecting mutant AR is most active in a given tissue, for example, lysosomal in certain viscera *vs.* via the ubiquitination pathway in most neural tissues. Taken together, diffuse nuclear accumulation of mutant AR is apparently a cardinal pathogenetic process underlying neuronal dysfunction and eventual cell death, while cytoplasmic accumulation may also contribute to the pathophysiology of SBMA.

Molecular pathogenesis

Two mechanisms of the involvement of polyQ-expanded mutant AR in the pathogenesis of SBMA have been proposed: mutant AR acquires a toxic property, damaging motor neurones; or loss of normal AR function induces neuronal degeneration [71]. As androgens have trophic effects on neuronal cells, one can assume that loss of AR function may play a role in the pathogenesis of SBMA. Expansion of the polyQ tract mildly suppresses the transcriptional activities of AR, probably because it disrupts the interaction between the N-terminal transactivating domain of AR and transcriptional coactivators. Although this loss of function of AR may contribute to androgen insensitivity, a gain of toxic function of the mutant AR due to the expanded polyQ tract has been believed to play a pivotal role in the pathogenesis of SBMA. This hypothesis is supported by the observations that patients with severe testicular feminization lacking AR function and AR knockout mice do not have motor impairment [72]. Moreover, a transgenic mouse model expressing a protein composed of expanded polyQ driven by the human AR promoter demonstrated motor impairment, suggesting that the expanded polyQ protein is sufficient to induce the pathogenic process [73], whereas the male AR knock-in mouse model of SBMA has signs of androgen insensitivity such as decreased fertility, progressive abnormalities of germ cell maturation and the Sertoli cell cytoskeleton, and testicular atrophy [74]. However, a recent study revealed that the absence of endogenous normal AR protein in SBMA transgenic mice had deteriorative effects on neuromuscular and endocrine-reproductive features of these mice, although this mouse model expressing AR with expanded polyQ tract does not display signs of androgen insensitivity in the presence of the normal endogenous mouse *AR* gene [75]. Collectively, both the gain-of-function mutant protein toxicity and loss of normal AR protein function are the basis for motor neurone degeneration in SBMA, whereas impairment of AR function possibly causes signs of androgen insensitivity.

The fact that AR has a specific ligand, that is, testosterone, renders the pathogenesis of SBMA unique among polyQ diseases. An *in vitro* study using transfected COS cells showed that AR localized in the nucleus in the presence of testosterone, while AR remained largely in the cytoplasm in the absence of the hormone [76]. The AR is normally confined to a multiheteromeric inactive complex in the cell cytoplasm, and translocates into the nucleus in a ligand-dependent manner. Moreover, the half-life of AR is prolonged in the presence of its ligand, suggesting ligand-dependent stabilization of AR [76,77]. This intracellular trafficking and stabilization of AR appear to play important roles in the pathogenesis of SBMA.

We previously generated transgenic mice expressing the full-length human *AR* gene containing either 24 or 97 CAG repeats under the control of a cytomegalovirus enhancer and a chicken β-actin promoter [35]. This model recapitulated not only the neurologic disorder but also the phenotypic difference with gender which is a specific feature of SBMA. Mice that expressed *AR* with 97 CAG repeats (AR-97Q) exhibited progressive motor impairment, while none of the mice that expressed *AR* with 24 CAG repeats (AR-24Q) showed abnormal phenotypes [35]. The AR-97Q mice demonstrated small body size, short lifespan, progressive muscle atrophy, and weakness as well as reduced cage activity, all of which were markedly pronounced and accelerated in the male AR-97Q mice, but were either not observed or far less severe in the female AR-97Q mice. Western blot analysis revealed the transgenic AR protein smearing from the top of the gel in proteins isolated from the spinal cord, cerebrum, heart, muscle and pancreas. Although the male AR-97Q mice had greater amounts of smearing protein than their female counterparts, the female AR-97Q mice had a greater amount of monomeric AR protein. Diffuse nuclear staining of AR-97Q and less frequent NIs as detected by 1C2, were demonstrated in neurones of the spinal cord, cerebrum, cerebellum, brainstem, and dorsal root ganglia as well as in nonneuronal tissues such as the heart, muscles and pancreas. Male AR-97Q mice showed markedly more abundant diffuse nuclear staining and NIs than females, in agreement with the gender differences in symptoms and Western blot profile. Despite the profound gender difference in pathogenic AR protein expression, there was no significant difference in the mRNA level of

transgene expression between the male and female AR-97Q mice. Other laboratories have also generated various animal models expressing the full-length human AR with expanded polyQ tract, almost all of which display phenotypic expression of motor dysfunction with gender effects [78]. Ligand-dependent neurodegeneration has also been observed in a fruit fly model of SBMA [36]. These observations indicate that the ligand plays important roles in the gender difference of phenotypes, especially with regard to its interactions with mutant AR in the posttranscriptional stage.

Hormonal therapies

The dramatic gender difference of phenotypes led us to attempt hormonal interventions as a treatment for SBMA. First, we castrated male AR-97Q mice in order to reduce their testosterone level [35]. Next, leuprorelin, a potent luteinizing hormone-releasing hormone (LHRH) analogue, was administered subcutaneously to noncastrated AR-97Q mice [37]. Leuprorelin suppresses the release of the gonadotrophins, luteinizing hormone and follicle-stimulating hormone. Two to 4 weeks after the start of leuprorelin administration, the serum testosterone level decreased to the level achieved by surgical castration. Leuprorelin-treated male AR-97Q mice showed profound improvement of symptoms and histopathologic findings, and reduced nuclear localization of the mutant AR compared with the untreated, noncastrated male AR-97Q mice [35,37]. The body weight, motor function, and lifespan of male AR-97Q mice significantly improved by castration or leuprorelin administration. Western blot analysis and histopathologic studies revealed diminished nuclear accumulation of mutant AR in the male AR-97Q mice that had undergone castration or leuprorelin administration compared with that in untreated, noncastrated male AR-97Q mice. These results suggest that testosterone has toxic effects in AR-97Q mice by accelerating nuclear translocation of the mutant AR and promoting stabilization of the mutant AR protein. On the contrary, castration and leuprorelin administration each prevented nuclear localization and stabilization of the mutant AR by reducing the testosterone level. Nuclear localization of the mutant protein with expanded polyQ tract is likely to be important for inducing neuronal cell dysfunction and degeneration in the majority of polyQ diseases. It thus appears logical that a reduction in testosterone level improved the phenotypic expression of SBMA by preventing nuclear localization of the mutant AR. Testosterone deprivation reversed motor dysfunction in another transgenic mouse model of SBMA [79].

When leuprorelin was subcutaneously administered to male AR-97Q mice every 2 weeks starting at 5 weeks of age, leuprorelin initially increased the serum testosterone level by acting as an agonist at the LHRH receptor, but subsequently reduced it to an undetectable level. Leuprorelin-treated AR-97Q mice showed deterioration of body weight, gait and performance of the rotarod task at 8–9 weeks of age, during the time when the serum testosterone level initially increased through the agonistic effect of leuprorelin [37]. This elevation in testosterone level was transient and was followed by suppression of testosterone production and sustained reversibility of polyQ pathogenesis. Intriguingly, immunostaining of tail specimens, sampled from the same individual mouse, demonstrated an increase in the number of muscle fibres with nuclear 1C2 staining at 4 weeks of leuprorelin administration, although the number of muscle fibres with nuclear 1C2 staining decreased after another 4 weeks of treatment [37]. These results indicate that testosterone deprivation is sufficient to reverse both the symptomatic and pathologic phenotypes in AR-97Q mice.

Successful treatment of AR-97Q mice with leuprorelin led us to perform testosterone blockade therapies in SBMA patients [80]. In a preliminary open trial, treatment with leuprorelin for 6 months significantly reduced nuclear accumulation of mutant AR in the scrotal skin of SBMA patients, suggesting that androgen deprivation interrupts the pathogenic process of human SBMA [80]. Another trial on a larger scale is currently underway to verify the clinical benefits of leuprorelin in SBMA patients.

Hsp90-dependent pathogenesis

Heat shock protein (Hsp) 90, a molecular chaperone, is essential for the function and stability of the AR, the C-terminus of which has a high affinity for Hsp90. Hsp90 induces a conformational change in AR that is required for its nuclear translocation after ligand activation [24,81,82]. Hsp90 functions in multicomponent complexes of chaperone proteins including Hsp70, Hop, Cdc37 and p23, leading to the folding, activation and assembly of Hsp90 client proteins [83]. Two main Hsp90 complexes are thought to exist: one complex is a stabilizing form with Cdc37 and p23 and this complex stabilizes Hsp90 client proteins including AR, while the other

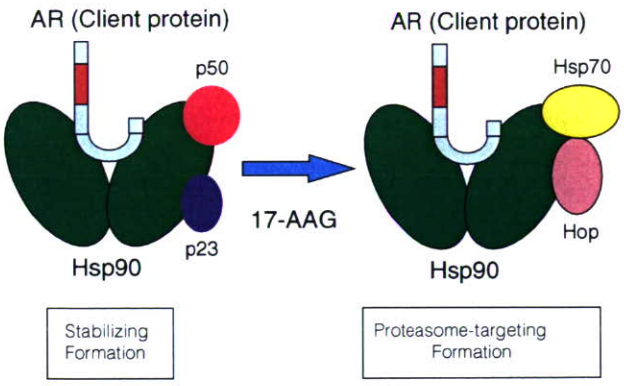

Figure 2. Diagram showing the change in the Hsp90 complex induced by an Hsp90 inhibitor. Hsp90 is required for nuclear translocation of androgen receptor (AR). Hsp90 functions in multicomponent complexes of cochaperone proteins including Hsp70, Hop, Cdc37 and p23. Two main Hsp90 complexes exist. One complex is a stabilizing form with Cdc37 and p23 and stabilizes Hsp90 client proteins, while the other complex is a proteasome-targeting form with Hsp70 and Hop and directs Hsp90 client proteins to proteasome degradation. Hsp90 inhibitor (17-AAG) specifically binds the ATP-binding site of Hsp90, resulting in a shift of the Hsp90 complex from the stabilizing form towards the proteasome-targeting form.

complex is a proteasome-targeting form with Hsp70 and Hop and it directs Hsp90 client proteins to proteasome degradation (Figure 2) [84–87]. p23 is thought to modulate Hsp90 activity during the last stages of the chaperoning pathway, leading to stabilization of Hsp90 client proteins in an ATP-dependent manner [88]. Hop is known to independently bind with both Hsp90 and Hsp70, thereby promoting the Hsp90/Hsp70 linkage, and is thought to direct the triage decision for client proteins by bridging the Hsp90–Hsp70 interaction [87]. Hsp90 inhibitors inhibit the ATP-dependent progression of the Hsp90 complex towards the stabilizing form and shift it to the proteasome-targeting form, resulting in proteasomal degradation of the Hsp90 client protein (Figure 2) [89,90]. Steroid receptors, including the progesterone receptor and the glucocorticoid receptor, were the first Hsp90 client proteins to be identified [91,92]. As for AR, Hsp90 is essential for maintaining its high ligand-binding affinity and for its stabilization [81,93]. In practice, Hsp90 inhibitors reduce the binding affinity of AR for androgens, and induce the degradation of AR [93,94]. Numerous oncoproteins belonging to the Hsp90 client protein family are selectively degraded in the UPS by Hsp90 inhibitors, and 17-allylamino-17-demethoxygeldanamycin (17-AAG), a first-in-class Hsp90 inhibitor, is now under clinical trials as a novel molecular-targeted agent for a wide range of malignancies [95]. In addition, Hsp90 inhibitors have been shown to have some neuroprotective effects against various stresses such as drug-induced toxicity, oxidative stress, and oxygen glucose deprivation [96–99]. AR also belongs to the Hsp90 client protein family, and is degraded in the presence of Hsp90 inhibitors [85,93,94]. Therefore, we explored the possibility of using 17-AAG as a therapeutic agent for neurodegenerative diseases by examining its effects on mutant AR in cultured cells and in a mouse model of SBMA. We found that 17-AAG inhibits nuclear accumulation of this protein in cultured cells, leading to marked amelioration of the motor phenotype of AR-97Q mice without detectable toxicity [100]. Of interest is the finding that 17-AAG preferentially targeted mutant AR rather than wild-type AR to proteasomal degradation. A high association between p23 and AR containing expanded polyQ tract renders the mutant AR more sensitive to Hsp90 inhibitors than wild-type AR [100]. Western blot and filter trap analyses in AR-97Q mice both showed that 17-AAG significantly reduced the amount of the insoluble high-molecular-weight complex of mutant AR as well as the amount of soluble monomer of mutant AR in the spinal cord and skeletal muscle. Moreover, in an immunostaining study of nervous tissue from AR-97Q mice, 17-AAG significantly reduced the amount of diffuse nuclear-accumulated AR, suggesting that 17-AAG had a curative effect on SBMA by reducing the amounts of oligomers and the soluble monomeric form of the mutant AR. Alternatively, 17-AAG may inhibit aggregation of mutant AR by inducing Hsp70 and Hsp40 expression. Hsp90 inhibitors cause disassociation of heat shock factor-1 (HSF-1) from the Hsp90 complex and trimerization of the HSF-1, thereby resulting in HSP activation [100]. The Hsp90 inhibitor, geldanamycin, induced Hsp70 and Hsp40 expression in transfected COS-1 cells, thereby inhibiting polyQ-induced abnormal aggregation of huntingtin protein [101]. However, as 17-AAG displayed only a limited ability to induce Hsp70 and Hsp40 expression in mouse tissue [100], the large decrease in the amount of AR seen in the insoluble fraction *in vivo*, rather than being a result of HSP induction, may be due to the potent ability of 17-AAG to degrade the soluble monomeric form of the mutant protein, thereby preventing its aggregation [100]. Furthermore, assembly of Hsp90 and its cofactors into complexes is required for retrograde, dynein-dependent movement of several steroid receptors [102,103]. Thus, in cells that do not express HSF-1, Hsp90 inhibitors inhibit the translocation of AR to the

nucleus and prevent ligand-dependent aggregation of the polyQ-expanded AR by inhibiting dynein-dependent AR trafficking [104].

Among the other proposed therapeutic approaches we previously studied [35,37,105,106], the efficacy of 17-AAG most closely approximated the successful hormonal therapy using the LH-RH analogue, leuprorelin [100]. However, unlike leuprorelin, the Hsp90 inhibitor 17-AAG holds enormous potential for application to a wide range of neurodegenerative diseases in addition to SBMA as previously reported [107–109]. We regard this general versatility as very important for the development of Hsp90 inhibitors as a treatment for neurological disorders. The strategy behind Hsp90 inhibitors differs from previous strategies employed against polyQ diseases, which unavoidably allowed abnormal protein to remain and placed much value mainly on inhibition of protein aggregation. We consider that the ability to facilitate degradation of disease-causing proteins by modulation of Hsp90 function would be of value when applied to SBMA and other neurodegenerative diseases. There is no doubt that reduction of the amount of the main culprit protein would have a curative effect against various neurodegenerative diseases. In fact, one therapeutic approach that directly reduces the level of abnormal protein by RNA interference has already proven beneficial in various mouse models of polyQ diseases and amyotrophic lateral sclerosis [110–112].

17-AAG-induced degradation requires a well-preserved proteasome function [89,90,100,113]. However, a question as to whether the UPS is impaired or not in patients with SBMA has been raised concerning this UPS-dependent therapy [113]. It is generally accepted that the UPS is involved in the pathology of polyQ diseases, as many components of the UPS and molecular chaperones are known to colocalize with polyQ-containing NIs [114,115]. Previous studies performed in cultured cell models suggested that the UPS is impaired in patients with polyQ diseases [54,116–118]. If this hypothesis were true, 17-AAG would not be able to exert its pharmacological effect on polyQ diseases. In this regard, recent studies using *in vivo* proteasome assays have raised important questions as to whether patients with polyQ diseases have an impaired UPS [53,119,120]. It has been reported that neuronal dysfunction developed without significant impairment of the UPS in a mouse model of SCA7 [53]. Consistent with this, it was also demonstrated that proteasome impairment did not contribute to the pathogenesis of HD in a mouse model [120]. Furthermore, in conditional mouse models of polyQ disease, genetic loss of the abnormal gene product led to rapid clearance of pre-existing polyQ-mediated NIs and reversible improvement of the abnormal phenotypes [121,122]. If the UPS were irreversibly damaged in patients and animal models of polyQ diseases, then the amount of pre-existing NIs would not decrease. We therefore consider that treatment with 17-AAG, which takes advantage of a self-clearing system to target disease-causing proteins, is a reasonable therapeutic strategy against polyQ-related and other neurodegenerative diseases.

Induction of heat shock proteins

Many components of the UPS and molecular chaperones are known to colocalize with polyQ-containing NIs, implying that these proteins are involved in neurodegeneration in polyQ diseases. HSPs are classified into different families according to molecular size: Hsp100, Hsp90, Hsp70, Hsp60, Hsp40 and small HSPs [123]. These HSPs are either constitutively expressed or inducibly synthesized after cellular stress. HSPs play important roles in maintaining correct folding, assembly, and intracellular transport of newly synthesized proteins. For example, Hsp70 and Hsp90, which are essential components of the AR–chaperone complex in the cell cytoplasm, regulate the function, nuclear translocation, and degradation of AR [124]. Under toxic conditions, the synthesis of HSPs is rapidly up-regulated, and nonnative proteins are refolded as a consequence. Therefore, forced overexpression of HSPs resulted in acquisition of tolerance against various types of stresses, and protection against apoptosis in various disease models [125]. In various polyQ disease models, both genetic and pharmacological overexpression of HSPs have been shown to suppress aggregate formation and cellular toxicity [109,114,126–128]. Hsp70 cooperates with Hsp40 in functioning as a molecular chaperone. These HSPs have been proposed to prevent the initial conformation conversion of mutant polyQ-containing protein from a random coil to a β-sheet, leading to attenuation of toxic oligomer formation [128]. Overexpression of Hsp70, together with Hsp40, inhibited the toxic accumulation of abnormal polyQ-containing protein and suppressed cell death in a variety of cellular models of polyQ diseases including SBMA [114,129]. Hsp70 has also been shown to facilitate proteasomal degradation of abnormal AR protein in a cell culture model of SBMA [130]. The favour-

able effects of Hsp70 have been verified in studies using mouse models of polyQ diseases. Overexpression of the inducible form of human Hsp70 markedly ameliorated the symptomatic and histopathological phenotypes of the SCA1 mouse model [131] and AR-97Q mice [105]. These beneficial effects were dependent on the dose of the Hsp70 gene and correlated with the reduction in the amount of nuclear-accumulated mutant AR protein [105]. It should be noted that Hsp70 overexpression also significantly reduced the amount of the soluble form of mutant AR, suggesting that Hsp70 overexpression accelerated the degradation of mutant AR in AR-97Q mice.

Favourable effects obtained by genetic modulation of HSPs suggest that pharmacological induction of molecular chaperones might be a promising approach for the treatment of SBMA and other polyQ diseases. Many studies have shown that HSP induction by Hsp90 inhibitors exerted potentially neuroprotective effects in models of HD [101,132,133], tauopathies [134–136], Parkinson's disease [137–139], stroke [140,141] and autoimmune encephalomyelitis [142]. As for polyQ diseases, Sittler *et al.* [101] first showed that geldanamycin significantly suppressed aggregation of mutant huntingtin in a cultured cell model of HD via induction of Hsp70 and Hsp40 heat shock response. Geranylgeranylacetone (GGA), an acyclic isoprenoid compound with a retinoid skeleton, has been shown to strongly induce HSP expression in various tissues [143]. This compound has been used as an oral anti-ulcer drug. Oral administration of GGA up-regulated the levels of Hsp70, Hsp90 and Hsp105 via activation of HSF-1 in the central nervous system and inhibited nuclear accumulation of the pathogenic AR protein, resulting in amelioration of polyQ-dependent neuromuscular phenotypes of the AR-97Q mice [144]. Thus, enhancement of cellular defences using Hsp90 inhibitors and GGA is a reasonable clinical approach for the treatment of neurodegenerative diseases. The ability of Hsp90 inhibitors to significantly induce the expression of HSPs has been demonstrated in cultured cells and a fly model, but not in mammals. As 17-AAG had only a limited ability to induce Hsp70 expression in mouse tissue [100], further studies should be performed to address to what extent Hsp90 inhibitors can induce the expression of HSPs in mouse models of neurodegenerative disorders other than SBMA.

On the other hand, several studies suggest that polyQ elongation interferes with the protective cellular responses against cytotoxic stress [128]. Transfected cells expressing truncated AR composed of the first N-terminal 127 amino acids of human AR with an expanded polyQ tract showed delayed induction of Hsp70 after heat shock compared with that in transfected cells expressing the full-length AR [145]. Bates and colleagues reported progressive decreases in the expression of Hsp70 and Hsp40 in the brain lesion of an animal model of HD [132], and such decreases were also observed in AR-97Q mice [144]. The threshold of HSP induction is known to be relatively high in spinal motor neurones [146]. Taken together, impairment of the capability of HSP induction is implicated in the pathogenesis of motor neurone degeneration in SBMA as HSPs are potent suppressors of polyQ toxicity.

Biomarkers for clinical trials

As SBMA is a slowly progressive disease and its precise natural history has not been well elucidated, long-term clinical trials are necessary to assess whether certain drugs can alter the natural progression of the disease. Suitable biomarkers that reflect the pathogenesis and severity of SBMA, are necessary to be able to assess the therapeutic efficacy and to improve the power and cost-effectiveness of longitudinal drug trials. Punch biopsy of the scrotal skin is safe and easy to perform on patients, whereas it is not practical to obtain a biopsy specimen from the central nervous system. We studied a biomarker of SBMA, that is, the degree of nuclear accumulation of mutant AR in epithelial cells of scrotal skin biopsy samples, which can be used as a surrogate endpoint in therapeutic trials [80]. In that study, the degree of nuclear accumulation of mutant AR in scrotal skin biopsy samples from 13 SBMA patients was assessed by 1C2 staining (Figure 1f). The percentage of cells with nuclear 1C2 staining among the scrotal skin epithelial cells tended to be correlated with that in spinal motor neurones among five autopsied SBMA cases, and it was positively correlated with the CAG repeat length and inversely correlated with the functional Activities of Daily Living scale as assessed by the Norris score on limbs among the 13 SBMA patients [80]. The results demonstrate that the percentage of cells with nuclear 1C2 staining in scrotal skin biopsy samples could predict the pathogenic process in the motor neurones of patients with SBMA. Moreover, subcutaneous injections of leuprorelin in SBMA patients reduced both the intensity and frequency of diffuse nuclear 1C2 staining in scrotal skin epithelial cells during the first 4 weeks of therapy and this effect was markedly enhanced after

12-week treatment, suggesting that 1C2 immunostaining of scrotal skin biopsy samples for nuclear mutant AR is a practical procedure for estimating the severity of SBMA pathogenesis in the nervous system [80]. Based on the observations described above, the degree of 1C2-stained nuclear mutant AR accumulation in biopsied scrotal skin is likely to be a potent biomarker reflecting the pathogenic process of SBMA. Since the degree of nuclear accumulation of mutant AR in biopsied scrotal skin appears to be a promising surrogate endpoint, further trials are necessary to evaluate this biomarker by confirming that the change in scrotal skin findings correctly predicts the true clinical outcome event such as becoming wheelchair-bound, aspiration pneumonia or death.

Conclusions

Studies using cellular and animal models provide insight into mechanisms involved in neurodegeneration in SBMA, and reveal promising approaches to treatment of this disease, among which LHRH analogues and 17-AAG appear to be potent agents for treating patients. The results of animal studies should be verified in carefully designed clinical trials. Clinical studies on SBMA patients, however, are challenging because of the slowly progressive nature of SBMA and the low sensitivity of clinical examination to detect changes over short periods of time. Furthermore, these treatments for SBMA are disease-modifying therapies that inhibit the pathogenic process of motor neurone degeneration rather than symptom-relief therapies (Figure 3). Therefore, large-scale clinical trials of long duration are necessary, and establishment of objective biomarkers is of utmost importance in order to improve the power and cost-effectiveness of longitudinal clinical treatment trials (Figure 3). For this purpose, clinical and pathological parameters representing the pathogenic process of SBMA should be extensively investigated.

The ideal treatment for polyQ diseases appears to be a combination of several potential therapeutic strategies, as each approach has adverse effects and long-term treatment is unavoidable in the therapy of polyQ diseases. Elucidation of the pathophysiology, high-throughput drug screening and intensive clinical trials are necessary for establishing human therapeutics for this disease.

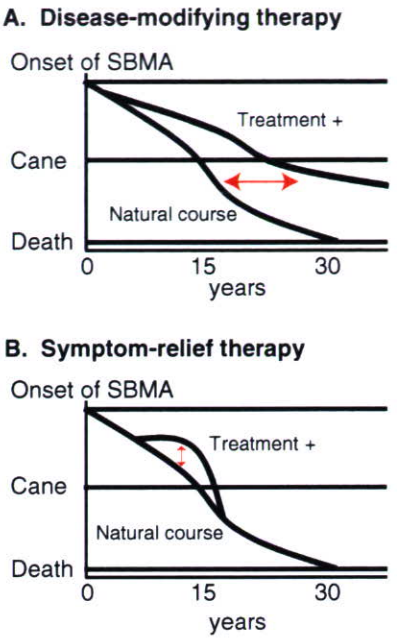

Figure 3. Disease-modifying and symptom-relief therapies for spinal and bulbar muscular atrophy (SBMA). (**A**) Long-term clinical trials are necessary to evaluate the effects of disease-modifying therapies, as SBMA is a slowly progressive disease. (**B**) Symptom-relief therapy ameliorates symptoms of SBMA, and the duration of these clinical trials is short. The *y*-axis shows the general clinical course of SBMA patients. 'Cane' indicates the requirement of a cane for walking. Arrows indicate the study duration that is required for each therapy.

Acknowledgements

We thank the National Cancer Institute and Kosan Biosciences for kindly providing 17-AAG. This work was supported by a Center-of-Excellence (COE) grant and KAKENHI (17025020) from the Ministry of Education, Culture, Sports, Science and Technology, Japan, grants from the Ministry of Health, Labour and Welfare, Japan, a grant from the Naito Foundation, and a grant from the Kanae Foundation.

References

1 Takahashi A. Hiroshi Kawahara (1858–1918). *J Neurol* 2001; **248**: 241–2
2 Kawahara H. A family of progressive bulbar palsy. *Aichi Med J* 1897; **16**: 3–4
3 Kennedy WR, Alter M, Sung JH. Progressive proximal spinal and bulbar muscular atrophy of late onset. A sex-linked recessive trait. *Neurology* 1968; **18**: 671–80
4 La Spada AR, Wilson EM, Lubahn DB, Harding AE, Fischbeck KH. Androgen receptor gene mutations in X-linked spinal and bulbar muscular atrophy. *Nature* 1991; **352**: 77–9
5 Di Prospero NA, Fischbeck KH. Therapeutics development for triplet repeat expansion diseases. *Nat Rev Genet* 2005; **6**: 756–65

6 Sobue G, Hashizume Y, Mukai E, Hirayama M, Mitsuma T, Takahashi A. X-linked recessive bulbospinal neuronopathy. A clinicopathological study. *Brain* 1989; **112**: 209–32
7 Lee JH, Shin JH, Park KP, Kim IJ, Kim CM, Lim JG, Choi YC, Kim DS. Phenotypic variability in Kennedy's disease: implication of the early diagnostic features. *Acta Neurol Scand* 2005; **112**: 57–63
8 Atsuta N, Watanabe H, Ito M, Banno H, Suzuki K, Katsuno M, Tanaka F, Tamakoshi A, Sobue G. Natural history of spinal and bulbar muscular atrophy (SBMA). A study of 223 Japanese patients. *Brain* 2006; **129**: 1446–55
9 Arbizu T, Santamaria J, Gomez JM, Quilez A, Serra JP. A family with adult spinal and bulbar muscular atrophy, X-linked inheritance and associated testicular failure. *J Neurol Sci* 1983; **59**: 371–82
10 Hausmanowa-Petrusewicz I, Borkowska J, Janczewski Z. X-linked adult form of spinal muscular atrophy. *J Neurol* 1983; **229**: 175–88
11 Nagashima T, Seko K, Hirose K, Mannen T, Yoshimura S, Arima R, Nagashima K, Morimatsu Y. Familial bulbospinal muscular atrophy associated with testicular atrophy and sensory neuropathy (Kennedy–Alter–Sung syndrome). Autopsy case report of two brothers. *J Neurol Sci* 1988; **87**: 141–52
12 Echaniz-Laguna A, Rousso E, Anheim M, Cossee M, Tranchant C. A family with early-onset and rapidly progressive X-linked spinal and bulbar muscular atrophy. *Neurology* 2005; **64**: 1458–60
13 Danek A, Witt TN, Mann K, Schweikert HU, Romalo G, La Spada AR, Fischbeck KH. Decrease in androgen binding and effect of androgen treatment in a case of X-linked bulbospinal neuronopathy. *Clin Invest* 1994; **72**: 892–7
14 Goldenberg JN, Bradley WG. Testosterone therapy and the pathogenesis of Kennedy's disease (X-linked bulbospinal muscular atrophy). *J Neurol Sci* 1996; **135**: 158–61
15 Neuschmid-Kaspar F, Gast A, Peterziel H, Schneikert J, Muigg A, Ransmayr G, Klocker H, Bartsch G, Cato AC. CAG-repeat expansion in androgen receptor in Kennedy's disease is not a loss of function mutation. *Mol Cell Endocrinol* 1996; **117**: 149–56
16 Antonini G, Gragnani F, Romaniello A, Pennisi EM, Morino S, Ceschin V, Santoro L, Cruccu G. Sensory involvement in spinal-bulbar muscular atrophy (Kennedy's disease). *Muscle Nerve* 2000; **23**: 252–8
17 Lieberman AP, Fischbeck KH. Triplet repeat expansion in neuromuscular disease. *Muscle Nerve* 2000; **23**: 843–50
18 Sinnreich M, Sorenson EJ, Klein CJ. Neurologic course, endocrine dysfunction and triplet repeat size in spinal bulbar muscular atrophy. *Can J Neurol Sci* 2004; **31**: 378–82
19 Schmidt BJ, Greenberg CR, Allingham-Hawkins DJ, Spriggs EL. Expression of X-linked bulbospinal muscular atrophy (Kennedy disease) in two homozygous women. *Neurology* 2002; **59**: 770–2
20 Sobue G, Doyu M, Kachi T, Yasuda T, Mukai E, Kumagai T, Mitsuma T. Subclinical phenotypic expressions in heterozygous females of X-linked recessive bulbospinal neuronopathy. *J Neurol Sci* 1993; **117**: 74–8
21 Greenland KJ, Zajac JD. Kennedy's disease: pathogenesis and clinical approaches. *Intern Med J* 2004; **34**: 279–86
22 Mariotti C, Castellotti B, Pareyson D, Testa D, Eoli M, Antozzi C, Silani V, Marconi R, Tezzon F, Siciliano G, Marchini C, Gellera C, Donato SD. Phenotypic manifestations associated with CAG-repeat expansion in the androgen receptor gene in male patients and heterozygous females: a clinical and molecular study of 30 families. *Neuromuscul Disord* 2000; **10**: 391–7
23 Sperfeld AD, Karitzky J, Brummer D, Schreiber H, Haussler J, Ludolph AC, Hanemann CO. X-linked bulbospinal neuronopathy: Kennedy disease. *Arch Neurol* 2002; **59**: 1921–6
24 Poletti A. The polyglutamine tract of androgen receptor: from functions to dysfunctions in motor neurons. *Front Neuroendocrinol* 2004; **25**: 1–26
25 Benten WP, Lieberherr M, Stamm O, Wrehlke C, Guo Z, Wunderlich F. Testosterone signaling through internalizable surface receptors in androgen receptor-free macrophages. *Mol Biol Cell* 1999; **10**: 3113–23
26 Lutz LB, Jamnongjit M, Yang WH, Jahani D, Gill A, Hammes SR. Selective modulation of genomic and nongenomic androgen responses by androgen receptor ligands. *Mol Endocrinol* 2003; **17**: 1106–16
27 Walker WH. Nongenomic actions of androgen in Sertoli cells. *Curr Top Dev Biol* 2003; **56**: 25–53
28 Ntais C, Polycarpou A, Tsatsoulis A. Molecular epidemiology of prostate cancer: androgens and polymorphisms in androgen-related genes. *Eur J Endocrinol* 2003; **149**: 469–77
29 Tanaka F, Doyu M, Ito Y, Matsumoto M, Mitsuma T, Abe K, Aoki M, Itoyama Y, Fischbeck KH, Sobue G. Founder effect in spinal and bulbar muscular atrophy (SBMA). *Hum Mol Genet* 1996; **5**: 1253–7
30 Tanaka F, Reeves MF, Ito Y, Matsumoto M, Li M, Miwa S, Inukai A, Yamamoto M, Doyu M, Yoshida M, Hashizume Y, Terao S, Mitsuma T, Sobue G. Tissue-specific somatic mosaicism in spinal and bulbar muscular atrophy is dependent on CAG-repeat length and androgen receptor – gene expression level. *Am J Hum Genet* 1999; **65**: 966–73
31 La Spada AR, Roling DB, Harding AE, Warner CL, Spiegel R, Hausmanowa-Petrusewicz I, Yee WC, Fischbeck KH. Meiotic stability and genotype-phenotype correlation of the trinucleotide repeat in X-linked spinal and bulbar muscular atrophy. *Nat Genet* 1992; **2**: 301–4

32 Igarashi S, Tanno Y, Onodera O, Yamazaki M, Sato S, Ishikawa A, Miyatani N, Nagashima M, Ishikawa Y, Sahashi K, Ibi T, Miyatake T, Tsuji S. Strong correlation between the number of CAG repeats in androgen receptor genes and the clinical onset of features of spinal and bulbar muscular atrophy. *Neurology* 1992; **42**: 2300–2

33 Doyu M, Sobue G, Mukai E, Kachi T, Yasuda T, Mitsuma T, Takahashi A. Severity of X-linked recessive bulbospinal neuronopathy correlates with size of the tandem CAG repeat in androgen receptor gene. *Ann Neurol* 1992; **32**: 707–10

34 Shimada N, Sobue G, Doyu M, Yamamoto K, Yasuda T, Mukai E, Kachi T, Mitsuma T. X-linked recessive bulbospinal neuronopathy: clinical phenotypes and CAG repeat size in androgen receptor gene. *Muscle Nerve* 1995; **18**: 1378–84

35 Katsuno M, Adachi H, Kume A, Li M, Nakagomi Y, Niwa H, Sang C, Kobayashi Y, Doyu M, Sobue G. Testosterone reduction prevents phenotypic expression in a transgenic mouse model of spinal and bulbar muscular atrophy. *Neuron* 2002; **35**: 843–54

36 Takeyama K, Ito S, Yamamoto A, Tanimoto H, Furutani T, Kanuka H, Miura M, Tabata T, Kato S. Androgen-dependent neurodegeneration by polyglutamine-expanded human androgen receptor in Drosophila. *Neuron* 2002; **35**: 855–64

37 Katsuno M, Adachi H, Doyu M, Minamiyama M, Sang C, Kobayashi Y, Inukai A, Sobue G. Leuprorelin rescues polyglutamine-dependent phenotypes in a transgenic mouse model of spinal and bulbar muscular atrophy. *Nat Med* 2003; **9**: 768–73

38 Sobue G, Matsuoka Y, Mukai E, Takayanagi T, Sobue I, Hashizume Y. Spinal and cranial motor nerve roots in amyotrophic lateral sclerosis and X-linked recessive bulbospinal muscular atrophy: morphometric and teased-fiber study. *Acta Neuropathol (Berl)* 1981; **55**: 227–35

39 Li M, Sobue G, Doyu M, Mukai E, Hashizume Y, Mitsuma T. Primary sensory neurons in X-linked recessive bulbospinal neuropathy: histopathology and androgen receptor gene expression. *Muscle Nerve* 1995; **18**: 301–8

40 Guidetti D, Vescovini E, Motti L, Ghidoni E, Gemignani F, Marbini A, Patrosso MC, Ferlini A, Solime F. X-linked bulbar and spinal muscular atrophy, or Kennedy disease: clinical, neurophysiological, neuropathological, neuropsychological and molecular study of a large family. *J Neurol Sci* 1996; **135**: 140–8

41 Li M, Miwa S, Kobayashi Y, Merry DE, Yamamoto M, Tanaka F, Doyu M, Hashizume Y, Fischbeck KH, Sobue G. Nuclear inclusions of the androgen receptor protein in spinal and bulbar muscular atrophy. *Ann Neurol* 1998; **44**: 249–54

42 Li M, Nakagomi Y, Kobayashi Y, Merry DE, Tanaka F, Doyu M, Mitsuma T, Hashizume Y, Fischbeck KH, Sobue G. Nonneural nuclear inclusions of androgen receptor protein in spinal and bulbar muscular atrophy. *Am J Pathol* 1998; **153**: 695–701

43 Kobayashi Y, Miwa S, Merry DE, Kume A, Mei L, Doyu M, Sobue G. Caspase-3 cleaves the expanded androgen receptor protein of spinal and bulbar muscular atrophy in a polyglutamine repeat length-dependent manner. *Biochem Biophys Res Commun* 1998; **252**: 145–50

44 Ellerby LM, Hackam AS, Propp SS, Ellerby HM, Rabizadeh S, Cashman NR, Trifiro MA, Pinsky L, Wellington CL, Salvesen GS, Hayden MR, Bredesen DE. Kennedy's disease: caspase cleavage of the androgen receptor is a crucial event in cytotoxicity. *J Neurochem* 1999; **72**: 185–95

45 Tanaka M, Machida Y, Nishikawa Y, Akagi T, Hashikawa T, Fujisawa T, Nukina N. Expansion of polyglutamine induces the formation of quasi-aggregate in the early stage of protein fibrillization. *J Biol Chem* 2003; **278**: 34717–24

46 Tanaka M, Morishima I, Akagi T, Hashikawa T, Nukina N. Intra- and intermolecular beta-pleated sheet formation in glutamine-repeat inserted myoglobin as a model for polyglutamine diseases. *J Biol Chem* 2001; **276**: 45470–5

47 Michalik A, Van Broeckhoven C. Pathogenesis of polyglutamine disorders: aggregation revisited. *Hum Mol Genet* 2003; **12**: R173–86

48 Simeoni S, Mancini MA, Stenoien DL, Marcelli M, Weigel NL, Zanisi M, Martini L, Poletti A. Motoneuronal cell death is not correlated with aggregate formation of androgen receptors containing an elongated polyglutamine tract. *Hum Mol Genet* 2000; **9**: 133–44

49 Bates G. Huntingtin aggregation and toxicity in Huntington's disease. *Lancet* 2003; **361**: 1642–4

50 Walcott JL, Merry DE. Trinucleotide repeat disease. The androgen receptor in spinal and bulbar muscular atrophy. *Vitam Horm* 2002; **65**: 127–47

51 Ross CA, Poirier MA, Wanker EE, Amzel M. Polyglutamine fibrillogenesis: the pathway unfolds. *Proc Natl Acad Sci USA* 2003; **100**: 1–3

52 Arrasate M, Mitra S, Schweitzer ES, Segal MR, Finkbeiner S. Inclusion body formation reduces levels of mutant huntingtin and the risk of neuronal death. *Nature* 2004; **431**: 805–10

53 Bowman AB, Yoo SY, Dantuma NP, Zoghbi HY. Neuronal dysfunction in a polyglutamine disease model occurs in the absence of ubiquitin-proteasome system impairment and inversely correlates with the degree of nuclear inclusion formation. *Hum Mol Genet* 2005; **14**: 679–91

54 Rusmini P, Sau D, Crippa V, Palazzolo I, Simonini F, Onesto E, Martini L, Poletti A. Aggregation and proteasome. The case of elongated polyglutamine aggregation in spinal and bulbar muscular atrophy. *Neurobiol Aging* 2006; doi: 10.1016/j.neurobiolaging.2006.05.015

55 Klement IA, Skinner PJ, Kaytor MD, Yi H, Hersch SM, Clark HB, Zoghbi HY, Orr HT. Ataxin-1 nuclear localization and aggregation: role in polyglutamine-induced disease in SCA1 transgenic mice. *Cell* 1998; **95**: 41–53

56 Saudou F, Finkbeiner S, Devys D, Greenberg ME. Huntingtin acts in the nucleus to induce apoptosis but death does not correlate with the formation of intranuclear inclusions. *Cell* 1998; **95**: 55–66
57 Yamada M, Wood JD, Shimohata T, Hayashi S, Tsuji S, Ross CA, Takahashi H. Widespread occurrence of intranuclear atrophin-1 accumulation in the central nervous system neurons of patients with dentatorubral-pallidoluysian atrophy. *Ann Neurol* 2001; **49**: 14–23
58 Adachi H, Katsuno M, Minamiyama M, Waza M, Sang C, Nakagomi Y, Kobayashi Y, Tanaka F, Doyu M, Inukai A, Yoshida M, Hashizume Y, Sobue G. Widespread nuclear and cytoplasmic accumulation of mutant androgen receptor in SBMA patients. *Brain* 2005; **128**: 659–70
59 Sapp E, Schwarz C, Chase K, Bhide PG, Young AB, Penney J, Vonsattel JP, Aronin N, DiFiglia M. Huntingtin localization in brains of normal and Huntington's disease patients. *Ann Neurol* 1997; **42**: 604–12
60 Garden GA, Libby RT, Fu YH, Kinoshita Y, Huang J, Possin DE, Smith AC, Martinez RA, Fine GC, Grote SK, Ware CB, Einum DD, Morrison RS, Ptacek LJ, Sopher BL, La Spada AR. Polyglutamine-expanded ataxin-7 promotes non-cell-autonomous purkinje cell degeneration and displays proteolytic cleavage in ataxic transgenic mice. *J Neurosci* 2002; **22**: 4897–905
61 Watase K, Weeber EJ, Xu B, Antalffy B, Yuva-Paylor L, Hashimoto K, Kano M, Atkinson R, Sun Y, Armstrong DL, Sweatt JD, Orr HT, Paylor R, Zoghbi HY. A long CAG repeat in the mouse Sca1 locus replicates SCA1 features and reveals the impact of protein solubility on selective neurodegeneration. *Neuron* 2002; **34**: 905–19
62 Yoo SY, Pennesi ME, Weeber EJ, Xu B, Atkinson R, Chen S, Armstrong DL, Wu SM, Sweatt JD, Zoghbi HY. SCA7 knockin mice model human SCA7 and reveal gradual accumulation of mutant ataxin-7 in neurons and abnormalities in short-term plasticity. *Neuron* 2003; **37**: 383–401
63 Steffan JS, Kazantsev A, Spasic-Boskovic O, Greenwald M, Zhu YZ, Gohler H, Wanker EE, Bates GP, Housman DE, Thompson LM. The Huntington's disease protein interacts with p53 and CREB-binding protein and represses transcription. *Proc Natl Acad Sci USA* 2000; **97**: 6763–8
64 Nucifora FC Jr, Sasaki M, Peters MF, Huang H, Cooper JK, Yamada M, Takahashi H, Tsuji S, Troncoso J, Dawson VL, Dawson TM, Ross CA. Interference by huntingtin and atrophin-1 with cbp-mediated transcription leading to cellular toxicity. *Science* 2001; **291**: 2423–8
65 Huynh DP, Yang HT, Vakharia H, Nguyen D, Pulst SM. Expansion of the polyQ repeat in ataxin-2 alters its Golgi localization, disrupts the Golgi complex and causes cell death. *Hum Mol Genet* 2003; **12**: 1485–96
66 Yamada M, Tsuji S, Takahashi H. Involvement of lysosomes in the pathogenesis of CAG repeat diseases. *Ann Neurol* 2002; **52**: 498–503
67 Taylor JP, Tanaka F, Robitschek J, Sandoval CM, Taye A, Markovic-Plese S, Fischbeck KH. Aggresomes protect cells by enhancing the degradation of toxic polyglutamine-containing protein. *Hum Mol Genet* 2003; **12**: 749–57
68 Ravikumar B, Duden R, Rubinsztein DC. Aggregate-prone proteins with polyglutamine and polyalanine expansions are degraded by autophagy. *Hum Mol Genet* 2002; **11**: 1107–17
69 Kegel KB, Kim M, Sapp E, McIntyre C, Castano JG, Aronin N, DiFiglia M. Huntingtin expression stimulates endosomal-lysosomal activity, endosome tubulation, and autophagy. *J Neurosci* 2000; **20**: 7268–78
70 Ishisaka R, Utsumi T, Yabuki M, Kanno T, Furuno T, Inoue M, Utsumi K. Activation of caspase-3-like protease by digitonin-treated lysosomes. *FEBS Lett* 1998; **435**: 233–6
71 Gatchel JR, Zoghbi HY. Diseases of unstable repeat expansion: mechanisms and common principles. *Nat Rev Genet* 2005; **6**: 743–55
72 Yeh S, Tsai MY, Xu Q, Mu XM, Lardy H, Huang KE, Lin H, Yeh SD, Altuwaijri S, Zhou X, Xing L, Boyce BF, Hung MC, Zhang S, Gan L, Chang C. Generation and characterization of androgen receptor knockout (ARKO) mice: an in vivo model for the study of androgen functions in selective tissues. *Proc Natl Acad Sci USA* 2002; **99**: 13498–503
73 Adachi H, Kume A, Li M, Nakagomi Y, Niwa H, Do J, Sang C, Kobayashi Y, Doyu M, Sobue G. Transgenic mice with an expanded CAG repeat controlled by the human AR promoter show polyglutamine nuclear inclusions and neuronal dysfunction without neuronal cell death. *Hum Mol Genet* 2001; **10**: 1039–48
74 Yu Z, Dadgar N, Albertelli M, Scheller A, Albin RL, Robins DM, Lieberman AP. Abnormalities of germ cell maturation and sertoli cell cytoskeleton in androgen receptor 113 CAG knock-in mice reveal toxic effects of the mutant protein. *Am J Pathol* 2006; **168**: 195–204
75 Thomas PS Jr, Fraley GS, Damien V, Woodke LB, Zapata F, Sopher BL, Plymate SR, La Spada AR. Loss of endogenous androgen receptor protein accelerates motor neuron degeneration and accentuates androgen insensitivity in a mouse model of X-linked spinal and bulbar muscular atrophy. *Hum Mol Genet* 2006; **15**: 2225–38
76 Kemppainen JA, Lane MV, Sar M, Wilson EM. Androgen receptor phosphorylation, turnover, nuclear transport, and transcriptional activation. Specificity for steroids and antihormones. *J Biol Chem* 1992; **267**: 968–74
77 Lieberman AP, Harmison G, Strand AD, Olson JM, Fischbeck KH. Altered transcriptional regulation in cells expressing the expanded polyglutamine androgen receptor. *Hum Mol Genet* 2002; **11**: 1967–76
78 Merry DE. Animal models of Kennedy disease. *Neurorx* 2005; **2**: 471–9
79 Chevalier-Larsen ES, O'Brien CJ, Wang H, Jenkins SC, Holder L, Lieberman AP, Merry DE. Castration restores

function and neurofilament alterations of aged symptomatic males in a transgenic mouse model of spinal and bulbar muscular atrophy. *J Neurosci* 2004; **24**: 4778–86

80 Banno H, Adachi H, Katsuno M, Suzuki K, Atsuta N, Watanabe H, Tanaka F, Doyu M, Sobue G. Mutant androgen receptor accumulation in spinal and bulbar muscular atrophy scrotal skin: a pathogenic marker. *Ann Neurol* 2006; **59**: 520–6

81 Fang Y, Fliss AE, Robins DM, Caplan AJ. Hsp90 regulates androgen receptor hormone binding affinity in vivo. *J Biol Chem* 1996; **271**: 28697–702

82 Georget V, Terouanne B, Nicolas JC, Sultan C. Mechanism of antiandrogen action: key role of hsp90 in conformational change and transcriptional activity of the androgen receptor. *Biochemistry* 2002; **41**: 11824–31

83 Pratt WB, Toft DO. Regulation of signaling protein function and trafficking by the hsp90/hsp70-based chaperone machinery. *Exp Biol Med (Maywood)* 2003; **228**: 111–33

84 Sullivan W, Stensgard B, Caucutt G, Bartha B, McMahon N, Alnemri ES, Litwack G, Toft D. Nucleotides and two functional states of hsp90. *J Biol Chem* 1997; **272**: 8007–12

85 Neckers L. Heat shock protein 90 inhibition by 17-allylamino-17-demethoxygeldanamycin: a novel therapeutic approach for treating hormone-refractory prostate cancer. *Clin Cancer Res* 2002; **8**: 962–6

86 Egorin MJ, Zuhowski EG, Rosen DM, Sentz DL, Covey JM, Eiseman JL. Plasma pharmacokinetics and tissue distribution of 17-(allylamino)-17-demethoxygeldanamycin (NSC 330507) in CD2F1 mice1. *Cancer Chemother Pharmacol* 2001; **47**: 291–302

87 McClellan AJ, Scott MD, Frydman J. Folding and quality control of the VHL tumor suppressor proceed through distinct chaperone pathways. *Cell* 2005; **121**: 739–48

88 Felts SJ, Toft DO. p23, a simple protein with complex activities. *Cell Stress Chaperones* 2003; **8**: 108–13

89 Mimnaugh EG, Chavany C, Neckers L. Polyubiquitination and proteasomal degradation of the p185c-erbB-2 receptor protein-tyrosine kinase induced by geldanamycin. *J Biol Chem* 1996; **271**: 22796–801

90 Bonvini P, Dalla Rosa H, Vignes N, Rosolen A. Ubiquitination and proteasomal degradation of nucleophosmin-anaplastic lymphoma kinase induced by 17-allylamino-demethoxygeldanamycin: role of the co-chaperone carboxyl heat shock protein 70-interacting protein. *Cancer Res* 2004; **64**: 3256–64

91 Smith DF, Whitesell L, Nair SC, Chen S, Prapapanich V, Rimerman RA. Progesterone receptor structure and function altered by geldanamycin, an hsp90-binding agent. *Mol Cell Biol* 1995; **15**: 6804–12

92 Johnson JL, Toft DO. Binding of p23 and hsp90 during assembly with the progesterone receptor. *Mol Endocrinol* 1995; **9**: 670–8

93 Vanaja DK, Mitchell SH, Toft DO, Young CY. Effect of geldanamycin on androgen receptor function and stability. *Cell Stress Chaperones* 2002; **7**: 55–64

94 Solit DB, Zheng FF, Drobnjak M, Munster PN, Higgins B, Verbel D, Heller G, Tong W, Cordon-Cardo C, Agus DB, Scher HI, Rosen N. 17-Allylamino-17-demethoxygeldanamycin induces the degradation of androgen receptor and HER-2/neu and inhibits the growth of prostate cancer xenografts. *Clin Cancer Res* 2002; **8**: 986–93

95 Neckers L. Hsp90 inhibitors as novel cancer chemotherapeutic agents. *Trends Mol Med* 2002; **8**: S55–61

96 Xiao N, Callaway CW, Lipinski CA, Hicks SD, DeFranco DB. Geldanamycin provides posttreatment protection against glutamate-induced oxidative toxicity in a mouse hippocampal cell line. *J Neurochem* 1999; **72**: 95–101

97 Sano M. Radicicol and geldanamycin prevent neurotoxic effects of anti-cancer drugs on cultured embryonic sensory neurons. *Neuropharmacology* 2001; **40**: 947–53

98 Xu L, Ouyang YB, Giffard RG. Geldanamycin reduces necrotic and apoptotic injury due to oxygen-glucose deprivation in astrocytes. *Neurol Res* 2003; **25**: 697–700

99 Ouyang YB, Xu L, Giffard RG. Geldanamycin treatment reduces delayed CA1 damage in mouse hippocampal organotypic cultures subjected to oxygen glucose deprivation. *Neurosci Lett* 2005; **380**: 229–33

100 Waza M, Adachi H, Katsuno M, Minamiyama M, Sang C, Tanaka F, Inukai A, Doyu M, Sobue G. 17-AAG, an Hsp90 inhibitor, ameliorates polyglutamine-mediated motor neuron degeneration. *Nat Med* 2005; **11**: 1088–95

101 Sittler A, Lurz R, Lueder G, Priller J, Lehrach H, Hayer-Hartl MK, Hartl FU, Wanker EE. Geldanamycin activates a heat shock response and inhibits huntingtin aggregation in a cell culture model of Huntington's disease. *Hum Mol Genet* 2001; **10**: 1307–15

102 Harrell JM, Murphy PJ, Morishima Y, Chen H, Mansfield JF, Galigniana MD, Pratt WB. Evidence for glucocorticoid receptor transport on microtubules by dynein. *J Biol Chem* 2004; **279**: 54647–54

103 Wochnik GM, Ruegg J, Abel GA, Schmidt U, Holsboer F, Rein T. FK506-binding proteins 51 and 52 differentially regulate dynein interaction and nuclear translocation of the glucocorticoid receptor in mammalian cells. *J Biol Chem* 2005; **280**: 4609–16

104 Thomas M, Harrell JM, Morishima Y, Peng HM, Pratt WB, Lieberman AP. Pharmacologic and genetic inhibition of hsp90-dependent trafficking reduces aggregation and promotes degradation of the expanded glutamine androgen receptor without stress protein induction. *Hum Mol Genet* 2006; **15**: 1876–83

105 Adachi H, Katsuno M, Minamiyama M, Sang C, Pagoulatos G, Angelidis C, Kusakabe M, Yoshiki A, Kobayashi Y, Doyu M, Sobue G. Heat shock protein 70 chaperone

overexpression ameliorates phenotypes of the spinal and bulbar muscular atrophy transgenic mouse model by reducing nuclear-localized mutant androgen receptor protein. *J Neurosci* 2003; **23**: 2203–11

106 Minamiyama M, Katsuno M, Adachi H, Waza M, Sang C, Kobayashi Y, Tanaka F, Doyu M, Inukai A, Sobue G. Sodium butyrate ameliorates phenotypic expression in a transgenic mouse model of spinal and bulbar muscular atrophy. *Hum Mol Genet* 2004; **13**: 1183–92

107 Whitesell L, Bagatell R, Falsey R. The stress response: implications for the clinical development of hsp90 inhibitors. *Curr Cancer Drug Targets* 2003; **3**: 349–58

108 Kamal A, Boehm MF, Burrows FJ. Therapeutic and diagnostic implications of Hsp90 activation. *Trends Mol Med* 2004; **10**: 283–90

109 Muchowski PJ, Wacker JL. Modulation of neurodegeneration by molecular chaperones. *Nat Rev Neurosci* 2005; **6**: 11–22

110 Xia H, Mao Q, Eliason SL, Harper SQ, Martins IH, Orr HT, Paulson HL, Yang L, Kotin RM, Davidson BL. RNAi suppresses polyglutamine-induced neurodegeneration in a model of spinocerebellar ataxia. *Nat Med* 2004; **10**: 816–20

111 Harper SQ, Staber PD, He X, Eliason SL, Martins IH, Mao Q, Yang L, Kotin RM, Paulson HL, Davidson BL. RNA interference improves motor and neuropathological abnormalities in a Huntington's disease mouse model. *Proc Natl Acad Sci USA* 2005; **102**: 5820–5

112 Raoul C, Abbas-Terki T, Bensadoun JC, Guillot S, Haase G, Szulc J, Henderson CE, Aebischer P. Lentiviral-mediated silencing of SOD1 through RNA interference retards disease onset and progression in a mouse model of ALS. *Nat Med* 2005; **11**: 423–8

113 La Spada AR, Weydt P. Targeting toxic proteins for turnover. *Nat Med* 2005; **11**: 1052–3

114 Cummings CJ, Mancini MA, Antalffy B, DeFranco DB, Orr HT, Zoghbi HY. Chaperone suppression of aggregation and altered subcellular proteasome localization imply protein misfolding in SCA1. *Nat Genet* 1998; **19**: 148–54

115 Ciechanover A, Brundin P. The ubiquitin proteasome system in neurodegenerative diseases: sometimes the chicken, sometimes the egg. *Neuron* 2003; **40**: 427–46

116 Bence NF, Sampat RM, Kopito RR. Impairment of the ubiquitin-proteasome system by protein aggregation. *Science* 2001; **292**: 1552–5

117 Jana NR, Zemskov EA, Wang G, Nukina N. Altered proteasomal function due to the expression of polyglutamine-expanded truncated N-terminal huntingtin induces apoptosis by caspase activation through mitochondrial cytochrome c release. *Hum Mol Genet* 2001; **10**: 1049–59

118 Holmberg CI, Staniszewski KE, Mensah KN, Matouschek A, Morimoto RI. Inefficient degradation of truncated polyglutamine proteins by the proteasome. *EMBO J* 2004; **23**: 4307–18

119 Zhou H, Cao F, Wang Z, Yu ZX, Nguyen HP, Evans J, Li SH, Li XJ. Huntingtin forms toxic NH2-terminal fragment complexes that are promoted by the age-dependent decrease in proteasome activity. *J Cell Biol* 2003; **163**: 109–18

120 Bett JS, Goellner GM, Woodman B, Pratt G, Rechsteiner M, Bates GP. Proteasome impairment does not contribute to pathogenesis in R6/2 Huntington's disease mice: exclusion of proteasome activator REG{gamma} as a therapeutic target. *Hum Mol Genet* 2006; **15**: 33–44

121 Yamamoto A, Lucas JJ, Hen R. Reversal of neuropathology and motor dysfunction in a conditional model of Huntington's disease. *Cell* 2000; **101**: 57–66

122 Zu T, Duvick LA, Kaytor MD, Berlinger MS, Zoghbi HY, Clark HB, Orr HT. Recovery from polyglutamine-induced neurodegeneration in conditional SCA1 transgenic mice. *J Neurosci* 2004; **24**: 8853–61

123 Macario AJ, Conway de Macario E. Sick chaperones, cellular stress, and disease. *N Engl J Med* 2005; **353**: 1489–501

124 Heinlein CA, Chang C. Role of chaperones in nuclear translocation and transactivation of steroid receptors. *Endocrine* 2001; **14**: 143–9

125 Rokutan K, Hirakawa T, Teshima S, Nakano Y, Miyoshi M, Kawai T, Konda E, Morinaga H, Nikawa T, Kishi K. Implications of heat shock/stress proteins for medicine and disease. *J Med Invest* 1998; **44**: 137–47

126 Warrick JM, Chan HY, Gray-Board GL, Chai Y, Paulson HL, Bonini NM. Suppression of polyglutamine-mediated neurodegeneration in Drosophila by the molecular chaperone HSP70. *Nat Genet* 1999; **23**: 425–8

127 Wyttenbach A, Carmichael J, Swartz J, Furlong RA, Narain Y, Rankin J, Rubinsztein DC. Effects of heat shock, heat shock protein 40 (HDJ-2), and proteasome inhibition on protein aggregation in cellular models of Huntington's disease. *Proc Natl Acad Sci USA* 2000; **97**: 2898–903

128 Wyttenbach A. Role of heat shock proteins during polyglutamine neurodegeneration: mechanisms and hypothesis. *J Mol Neurosci* 2004; **23**: 69–96

129 Kobayashi Y, Kume A, Li M, Doyu M, Hata M, Ohtsuka K, Sobue G. Chaperones Hsp70 and Hsp40 suppress aggregate formation and apoptosis in cultured neuronal cells expressing truncated androgen receptor protein with expanded polyglutamine tract. *J Biol Chem* 2000; **275**: 8772–8

130 Bailey CK, Andriola IF, Kampinga HH, Merry DE. Molecular chaperones enhance the degradation of expanded polyglutamine repeat androgen receptor in a cellular model of spinal and bulbar muscular atrophy. *Hum Mol Genet* 2002; **11**: 515–23

131 Cummings CJ, Sun Y, Opal P, Antalffy B, Mestril R, Orr HT, Dillmann WH, Zoghbi HY. Over-expression of inducible HSP70 chaperone suppresses neuropathology and improves motor function in SCA1 mice. *Hum Mol Genet* 2001; **10**: 1511–18

132 Hay DG, Sathasivam K, Tobaben S, Stahl B, Marber M, Mestril R, Mahal A, Smith DL, Woodman B, Bates GP. Progressive decrease in chaperone protein levels in a mouse model of Huntington's disease and induction of stress proteins as a therapeutic approach. *Hum Mol Genet* 2004; **13**: 1389–405

133 Agrawal N, Pallos J, Slepko N, Apostol BL, Bodai L, Chang LW, Chiang AS, Thompson LM, Marsh JL. Identification of combinatorial drug regimens for treatment of Huntington's disease using Drosophila. *Proc Natl Acad Sci USA* 2005; **102**: 3777–81

134 Dou F, Netzer WJ, Tanemura K, Li F, Hartl FU, Takashima A, Gouras GK, Greengard P, Xu H. Chaperones increase association of tau protein with microtubules. *Proc Natl Acad Sci USA* 2003; **100**: 721–6

135 Petrucelli L, Dickson D, Kehoe K, Taylor J, Snyder H, Grover A, De Lucia M, McGowan E, Lewis J, Prihar G, Kim J, Dillmann WH, Browne SE, Hall A, Voellmy R, Tsuboi Y, Dawson TM, Wolozin B, Hardy J, Hutton M. CHIP and Hsp70 regulate tau ubiquitination, degradation and aggregation. *Hum Mol Genet* 2004; **13**: 703–14

136 Benussi L, Ghidoni R, Paterlini A, Nicosia F, Alberici AC, Signorini S, Barbiero L, Binetti G. Interaction between tau and alpha-synuclein proteins is impaired in the presence of P301L tau mutation. *Exp Cell Res* 2005; **308**: 78–84

137 Auluck PK, Bonini NM. Pharmacological prevention of Parkinson disease in Drosophila. *Nat Med* 2002; **8**: 1185–6

138 Auluck PK, Meulener MC, Bonini NM. Mechanisms of suppression of {alpha}-synuclein neurotoxicity by geldanamycin in Drosophila. *J Biol Chem* 2005; **280**: 2873–8

139 Flower TR, Chesnokova LS, Froelich CA, Dixon C, Witt SN. Heat shock prevents alpha-synuclein-induced apoptosis in a yeast model of Parkinson's disease. *J Mol Biol* 2005; **351**: 1081–100

140 Lu A, Ran R, Parmentier-Batteur S, Nee A, Sharp FR. Geldanamycin induces heat shock proteins in brain and protects against focal cerebral ischemia. *J Neurochem* 2002; **81**: 355–64

141 Giffard RG, Xu L, Zhao H, Carrico W, Ouyang Y, Qiao Y, Sapolsky R, Steinberg G, Hu B, Yenari MA. Chaperones, protein aggregation, and brain protection from hypoxic/ischemic injury. *J Exp Biol* 2004; **207**: 3213–20

142 Murphy P, Sharp A, Shin J, Gavrilyuk V, Dello Russo C, Weinberg G, Sharp FR, Lu A, Heneka MT, Feinstein DL. Suppressive effects of ansamycins on inducible nitric oxide synthase expression and the development of experimental autoimmune encephalomyelitis. *J Neurosci Res* 2002; **67**: 461–70

143 Hirakawa T, Rokutan K, Nikawa T, Kishi K. Geranylgeranylacetone induces heat shock proteins in cultured guinea pig gastric mucosal cells and rat gastric mucosa. *Gastroenterology* 1996; **111**: 345–57

144 Katsuno M, Sang C, Adachi H, Minamiyama M, Waza M, Tanaka F, Doyu M, Sobue G. Pharmacological induction of heat-shock proteins alleviates polyglutamine-mediated motor neuron disease. *Proc Natl Acad Sci USA* 2005; **102**: 16801–6

145 Cowan KJ, Diamond MI, Welch WJ. Polyglutamine protein aggregation and toxicity are linked to the cellular stress response. *Hum Mol Genet* 2003; **12**: 1377–91

146 Batulan Z, Shinder GA, Minotti S, He BP, Doroudchi MM, Nalbantoglu J, Strong MJ, Durham HD. High threshold for induction of the stress response in motor neurons is associated with failure to activate HSF1. *J Neurosci* 2003; **23**: 5789–98

Received 29 August 2006
Accepted after revision 18 December 2006

PAPER

Usefulness of combined fractional anisotropy and apparent diffusion coefficient values for detection of involvement in multiple system atrophy

Mizuki Ito, Hirohisa Watanabe, Yoshinari Kawai, Naoki Atsuta, Fumiaki Tanaka, Shinji Naganawa, Hiroshi Fukatsu, Gen Sobue

J Neurol Neurosurg Psychiatry 2007;**78**:722–728. doi: 10.1136/jnnp.2006.104075

See end of article for authors' affiliations

Correspondence to: Professor Gen Sobue, Department of Neurology, Nagoya University Graduate School of Medicine, 65 Tsurumai-cho Showa-ku, Nagoya 466-8550, Japan; sobueg@med.nagoya-u.ac.jp

Received 8 August 2006
Revised 12 February 2007
Accepted 4 March 2007
Published Online First 12 March 2007

Objective: To determine whether apparent diffusion coefficient (ADC) values and fractional anisotropy (FA) values can detect early pathological involvement in multiple system atrophy (MSA), and be used to differentiate MSA-P (multiple system atrophy if parkinsonian features predominate) from Parkinson's disease (PD).

Methods: We compared ADC and FA values in the pons, cerebellum and putamen of 61 subjects (20 probable MSA patients, 21 age matched PD patients and 20 age matched healthy controls) using a 3.0 T magnetic resonance system.

Results: ADC values in the pons, cerebellum and putamen were significantly higher, and FA values lower in MSA than in PD or controls. These differences were prominent in MSA lacking dorsolateral putaminal hyperintensity (DPH) or hot cross bun (HCB) sign. In differentiating MSA-P from PD using FA and ADC values, we obtained equal sensitivity (70%) and higher specificity (100%) in the pons than in the putamen and cerebellum. In addition, all patients that had both significant low FA and high ADC values in each of these three areas were MSA-P cases, and those that had both normal FA and ADC values in the pons were all PD cases. Our diagnostic algorithm based on these results accurately diagnosed 90% of patients with MSA-P.

Conclusion: FA and ADC values detected early pathological involvement prior to magnetic resonance signal changes in MSA. In particular, low FA values in the pons showed high specificity in discriminating MSA-P from PD. In addition, combined analysis of both FA and ADC values in all three areas was more useful than only one.

Multiple system atrophy (MSA) is a sporadic adult onset neurodegenerative disease presenting a combination of parkinsonism, cerebellar ataxia and autonomic failure during the course of the illness.[1–4] A consensus statement recommended designating patients as having MSA-P if parkinsonian features predominated or MSA-C if cerebellar features predominated.[5] Differentiation of Parkinson's disease (PD) from MSA-P is particularly important because these disorders differ in progression, prognosis and treatment responses.[6] However, a purely clinical differentiation, especially in the early phase of the disease, remains challenging.

In advanced MSA, MRI reliably shows characteristic signal changes, such as dorsolateral putaminal hyperintensity (DPH) and the hot cross bun (HCB) sign,[7–10] but these signs are not useful for differentiation between MSA-P and PD in their early phases.[11]

Apparent diffusion coefficient (ADC) values and fractional anisotropy (FA) values are new parameters on MRI, and these were used to evaluate the degree of tissue degeneration in various disorders. ADC values measure the average water diffusion, and increasing ADC values indicate tissue degeneration. FA values measure the degree of anisotropy of the diffusing water along different axes of the image, and decreasing FA values represent tissue degeneration. Recently, there have been some reports concerning ADC and FA values in MSA-P and PD patients. ADC values in the striatum were higher in MSA-P than in PD,[12] and those in the basis pontis and cerebellum were higher in MSA-C than in controls.[13] FA values in the middle cerebellar penduncle, basis pontis and internal capsule were lower in MSA-C than in controls.[14] However, these results still do not confirm whether ADC and FA values are really effective at discriminating MSA-P from PD, particularly in their early phases. To confirm the hypothesis that ADC and FA values can detect abnormalities in patients with MSA, even without DPH and HCB, and discriminate MSA-P from PD, a direct study of these values at various stages of MSA and PD and in various regions is needed.

The aim of the present investigation was to examine the utility of ADC and FA values in the pons, cerebellum and putamen to detect not only the early pathological changes in MSA but also to differentiate MSA-P from PD.

PATIENTS AND METHODS

We studied 61 subjects (20 consecutive patients with probable MSA (10 MSA-C; 10 MSA-P), 21 age and sex matched patients with probable PD and 20 age and sex matched healthy volunteers) (table 1). There was a significant difference in the duration from initial symptoms to MRI evaluation between MSA (4 (2) years, range 1–10) and PD (10 (8) years, range 1–30) patients. Furthermore, patients with MSA-P and PD were assessed using the Hohen–Yahr score. There was no significant difference in the Hohen–Yahr score between the MSA-P (3.6 (1.0)) and PD (3.5 (1.0)) groups. Patients in the relatively early stage of MSA were included in this study. Clinical diagnoses of MSA[5] and PD[15] were established by consensus diagnostic

Abbreviations: ADC, apparent diffusion coefficient; DPH, dorsolateral putaminal hyperintensity; FA, fractional anisotropy; HCB, hot cross bun; MSA, multiple system atrophy; MSA-C, multiple system atrophy if cerebellar features predominate; MSA-P, multiple system atrophy if parkinsonian features predominate; PD, Parkinson's disease; ROC, receiver operating characteristic; ROI, region of interest

Table 1 Patients data

	No of cases	Age (y)	Sex (F/M)	Duration (y)	H-Y
MSA	20	61 (9)	8/12	4 (2)	
MSA-P	10	63 (11)	4/6	4 (3)	3.6 (1.0)
MSA-C	10	58 (7)	4/6	4 (2)	
PD	21	62 (11)	13/8	10 (8)	3.5 (1.0)
Control	20	62 (11)	13/7		

ADC, apparent diffusion coefficient; DPH, dorsolateral putaminal hyperintensity; FA, fractional anisotropy; HCB, hot cross bun; MSA, multiple system atrophy; MSA-C, multiple system atrophy if cerebellar features predominate; MSA-P, multiple system atrophy if parkinsonian features predominate; PD, Parkinson's disease.

criteria. All MSA patients fulfilled clinically probable criteria. In addition, controls underwent the same MRI examination. Informed consent was established before subject participation. This study was approved by the ethics committee of the Nagoya University Graduate School of Medicine.

MRI protocol

All scanning was carried out with a 3.0 T MR scanner (Trio, Siemens, Erlangen, Germany), using a receive only 8 channel phased array head coil. Diffusion weighted imaging was obtained with optimal methods[16] using a Stejskal–Tanner sequence with single shot spin echo-type echo planar imaging, flip angle of 90° and a repetition time of 7700 ms. Echo times corresponding to respective b-factors were 75 ms for 700 s/mm^2. Echo spacing was 0.79 ms, and matrix size was 128×128 with a readout bandwidth of 1562 Hz/pixel. Sixty axial slices, 2 mm thick with a 0.6 mm interslice gap, were used to image the entire brain with a 23 cm square field of view.

A motion probing gradient was applied in six orientations after acquisition of b = 700 images. The 128×128 data matrix was zero fill interpolated to 256×256. An acceleration factor of 2 was applied using the parallel imaging technique, generalised autocalibrating partially parallel acquisitions (GRAPPA),[17] which is an extension of the simultaneous acquisition of spatial harmonics technique. Eddy current related geometric distortions were not prominent between the images of each motion probing gradient directions and thus distortion correction post-processing was not applied.

Data analyses

ADC and FA values, and tractography were obtained using the public domain software dTV II for diffusion weighted imaging analysis developed by the Imaging Computing and Analysis Laboratory (Department of Radiology, University of Tokyo Hospital, Japan), and made available via the URL http://www.ut-radiology.umin.jp/people/masutani/dTV.htm. Regions of interest (ROIs) in the pons and cerebellum were placed within closed curves drawn around the entire axially imaged pons and around the axial cerebellum section that showed the largest dentate nucleus profile (fig 1A, 1B). As it was difficult to discriminate the entire axial putamen on MRI, ROIs in the putamen were placed within closed fixed circles drawn on the axial putaminal section (fig 1C). Regional ADC and FA values were calculated in each ROI. Mean ADC and FA values were adapted as representative indices of ADC and FA values. For tractography visualisation in the pons and cerebellum, which could be anatomically analysed in their entirety, seed areas were defined on T2 weighted axial images (b = 0) as the interior of the previously mentioned closed curve drawn around the pons and cerebellum. The presence or absence of HCB or DPH signs[18] was determined on T2 weighted axial images of the pons or putamen by the radiologist.

Statistical analyses were performed using SPSS 11.0 for Windows (SPSS Inc, USA). The Kruskal–Wallis test was used for comparison of ADC or FA values among MSA, PD and controls or MSA-P, PD and controls. The significance level was set at $p<0.05$. In addition, to differentiate probable MSA-P from PD, we performed receiver operating characteristic (ROC) analysis for FA and ADC values in each ROI. Based on these ROC data, we set cut off points for FA and ADC values, respectively.

RESULTS

Features of tractography

Tractography in representative MSA, PD and control subjects is shown in fig 2. Compared with PD and controls, MSA showed a decreased volume of fibre bundles corresponding anatomically to the middle cerebellar peduncle, transverse pontine and pyramidal tract fibres located in the pontine ROI, and also to the middle cerebellar peduncle and frontocerebellar tract located in the cerebellar ROI. No marked difference was seen between PD and controls. Although these fibre bundle losses were prominent in most MSA patients, some MSA cases had relatively well preserved tractography.

FA and ADC values in the pons, cerebellum and putamen

FA values in the pons, cerebellum and putamen in MSA were significantly lower than those in PD or controls. With respect to MSA phenotype, FA values in all three areas were significantly lower in MSA-P and MSA-C than in either PD or controls (fig 3A–C). However, FA values in the pons and cerebellum tended to be lower in MSA-C than in MSA-P, but the differences were not significant. FA values in the putamen were similar in MSA-C and MSA-P subjects.

ADC values in the pons, cerebellum and putamen were significantly higher in MSA than in PD or controls. With respect to MSA phenotype, ADC values in all three areas were significantly higher in MSA-P or MSA-C than in PD or controls (fig 4A–C), while ADC values in the pons and cerebellum tended to be higher in MSA-C than in MSA-P, but the

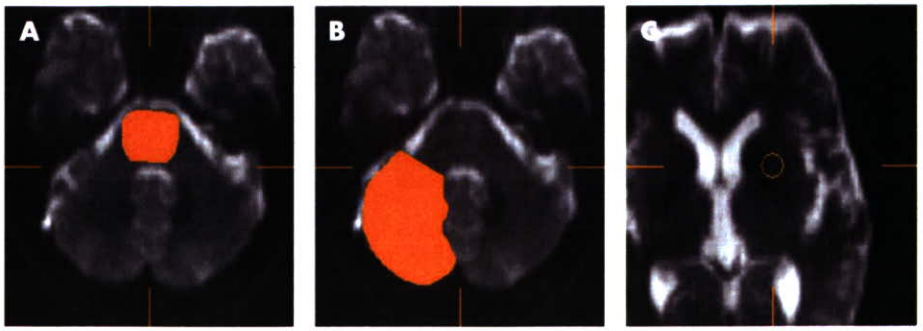

Figure 1 Regions of interest (ROI). ROIs in the pons (A), cerebellum (B) and putamen (C).

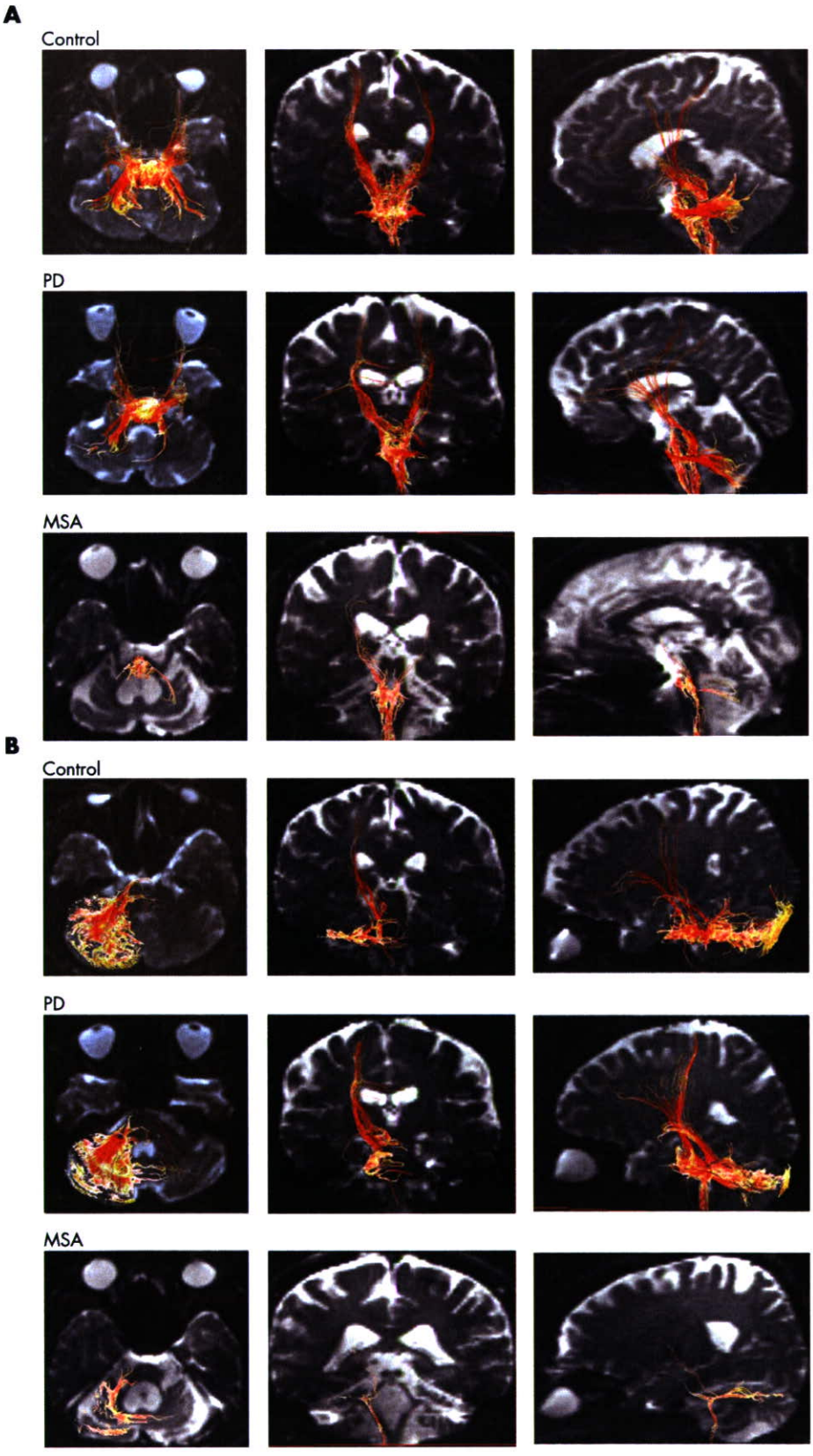

Figure 2 Tractography in the pons and cerebellum. (A) Pons. Visualisation of fibres in the pons and pyramidal tract fibres is unclear in multiple system atrophy (MSA). (B) Cerebellum. Visualisation of transverse fibres proceeding via the middle cerebellar peduncle, and of fibres connecting to the frontal lobe is unclear in MSA. PD, Parkinson's disease.

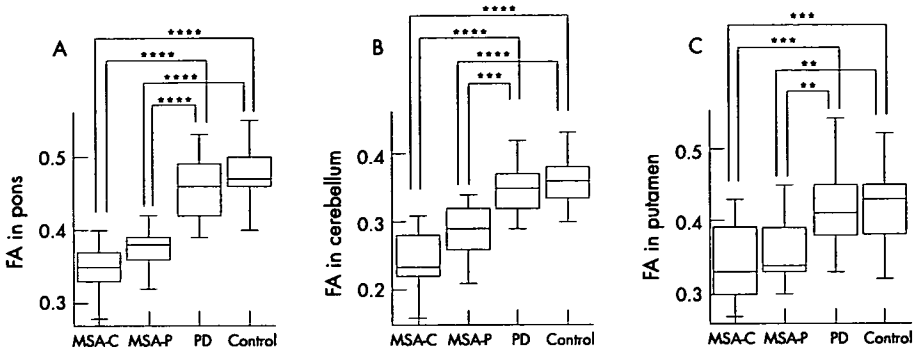

Figure 3 Fractional anisotropy (FA) values in the pons, cerebellum and putamen. FA values in multiple system atrophy if cerebellar features predominate (MSA-C), multiple system atrophy if parkinsonian features predominate (MSA-P), Parkinson's disease (PD) and controls are shown in the pons (A), cerebellum (B) and putamen (C). **p<0.01, ***p<0.005, ****p<0.001. FA values in all three areas were significantly lower in MSA-P and MSA-C than in PD or controls.

difference was not significant. ADC values in the putamen were similar in MSA-C and MSA-P.

Statistically lower FA and higher ADC values in the pons and cerebellum were more prominent than those in the putamen.

FA and ADC values in MSA with or without magnetic resonance signal changes

In our MSA patients, specificity of the HCB and DPH signs were both 100%, while sensitivity of the HCB and DPH signs were only 45.0% and 40.0%, respectively. However, in 11 MSA patients without the HCB sign, 8 (72.7%) showed low FA values in the pons, 7 (63.6%) in the cerebellum and 6 (54.5%) in the putamen, and 8 (72.7%) showed high ADC values in the pons, 6 (54.5%) in the cerebellum and 8 (72.7%) in the putamen (table 2). In 12 MSA patients without the DPH sign, 10 (83.3%) showed low FA values in the pons, 10 (83.3%) in the cerebellum and 10 (83.3%) in the putamen, and 8 (66.7%) showed high ADC values in the pons, 9 (75.0%) in the cerebellum and 6 (50.0%) in the putamen (table 2). These observations demonstrate that changes in FA and ADC values can be detected prior to the appearance of HCB and DPH signs in early phase MSA. FA values were significantly lower in MSA patients without DPH or HCB signs than in PD patients. Likewise, ADC values were significantly higher in MSA patients without DPH or HCB signs than in PD patients.

Differentiating MSA-P from PD

To differentiate probable MSA-P from PD, we performed ROC analysis. Based on these ROC data, we set cut off points for FA values in the pons, cerebellum and putamen at 0.38, 0.30 and 0.35, and for ADC values 0.98, 0.96 and 0.83, respectively, and that both sensitivity and specificity were as high as possible in our cases. Sensitivity and specificity based on these cut off points for FA values were 70.0% and 100.0% in the pons, 70.0% and 63.6% in the cerebellum and 70.0% and 87.5% in the putamen (fig 5). Sensitivity and specificity based on these cut off points for ADC values were 70.0% and 70.0% in the pons, 60.0% and 87.5% in the cerebellum and 70.0% and 63.6% in the putamen (fig 5). FA values in the pons were particularly useful for readily differentiating MSA-P from PD, and provided equal sensitivity and higher specificity than those in the cerebellum and putamen. Hence pontine FA values were especially useful markers to diagnose MSA-P as well as those in the cerebellum and putamen.

In addition, our results showed that three MSA-P patients had low FA but normal ADC values (fig 5A, red area) and three had normal FA but high ADC values (fig 5A, blue area) in the pons. In the cerebellum and putamen (fig 5B, C), two and two MSA-P patients, respectively, had low FA but normal ADC values, and one and two, respectively, had normal FA but high ADC values.

All patients that had both low FA and high ADC values in each of the three areas were probable MSA-P cases (fig 5A–C, purple areas), suggesting that patients with such values have a high possibility of being correctly diagnosed as MSA-P. Furthermore, no MSA cases had both normal FA and ADC values in the pons (fig 5A, white area), and all patients that had both normal FA and ADC values in the pons were PD cases. However, in the cerebellum and putamen (fig 5B, C, white areas), two and one MSA-P cases, respectively, had both normal FA and ADC values. Hence it was more useful to examine both FA and ADC values than only one or the other to distinguish MSA-P from PD.

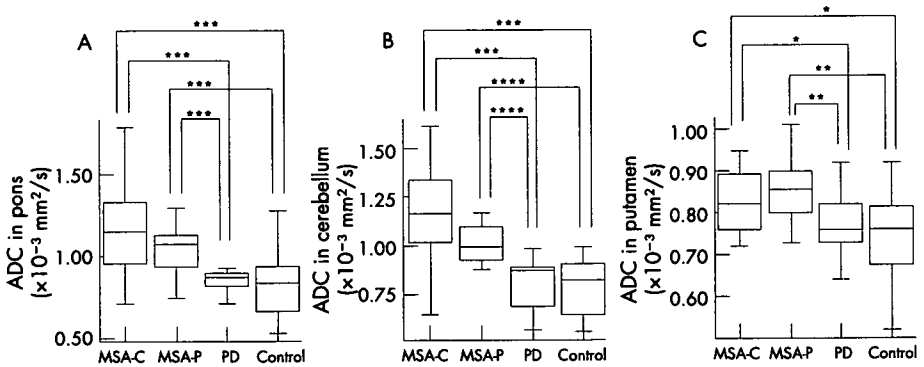

Figure 4 Apparent diffusion coefficient (ADC) values in the pons, cerebellum and putamen. ADC values ($\times 10^{-3}$ mm^2/s) in multiple system atrophy if cerebellar features predominate (MSA-C), multiple system atrophy if parkinsonian features predominate (MSA-P), Parkinson's disease (PD) and controls are shown in the pons (A), cerebellum (B) and putamen (C). *p<0.05, **p<0.01, ***p<0.005, ****p<0.001. ADC values in all three areas were significantly higher in MSA-P or MSA-C than in PD or controls.

Table 2 Percentage of patients with multiple system atrophy presenting with low fractional anisotropy or high apparent diffusion coefficient values without dorsolateral putaminal hyperintensity or hot cross bun signs

ROI	Cut off points	MSA patients without DPH sign (n = 12)	MSA patients without HCB sign (n = 11)
Pons			
	FA ≤0.38	10 (83.3%)	8 (72.7%)
	ADC ≥0.98	8 (66.7%)	8 (72.7%)
Cerebellum			
	FA ≤0.30	10 (83.3%)	7 (63.6%)
	ADC ≥0.96	9 (75.0%)	6 (54.5%)
Putamen			
	FA ≤0.35	10 (83.3%)	6 (54.5%)
	ADC ≥0.83	6 (50.0%)	8 (72.7%)

ADC, apparent diffusion coefficient; DPH, dorsolateral putaminal hyperintensity; FA, fractional anisotropy; HCB, hot cross bun; MSA, multiple system atrophy; ROI, region of interest.

Therefore, based on these results, we devised an algorithm for differentiating probable MSA-P from PD (fig 6). Using this algorithm in our 31 cases (PD 21; probable MSA-P 10), all patients that had both normal FA and ADC values in all three areas were PD cases (12 PD cases). In addition, all patients that had both low FA and high ADC values in any of the three areas were probable MSA-P cases (9 probable MSA-P cases). Taken together, the "MSA area" included 90.0% of probable MSA-P cases and no PD cases, and the "PD area" included 57.1% of PD cases and no probable MSA-P cases.

DISCUSSION

To our knowledge, this is the first systematic study to demonstrate the usefulness of simultaneous assessment of ADC and FA values on multiple regions, including the pons, cerebellum and putamen in MSA, PD and controls. We showed that low FA and high ADC values in these regions were significant even in MSA cases without HCB or DPH signs, suggesting that FA and ADC assessment can be a potent

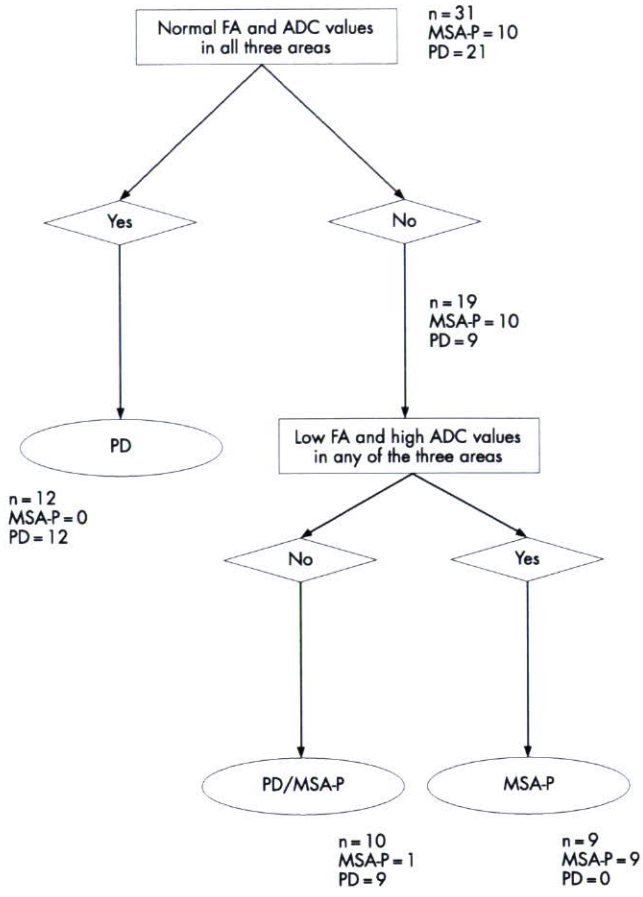

Figure 6 Algorithm for differentiating probable multiple system atrophy if parkinsonian features predominate (MSA-P) from Parkinson's disease (PD) using fractional anisotropy (FA) and apparent diffusion coefficient (ADC) values. Using this algorithm in our 31 cases (PD 21; probable MSA-P 10), the "MSA area" included 90% of probable MSA-P cases and no PD cases, and the "PD area" included 57.1% of PD cases and no MSA-P cases.

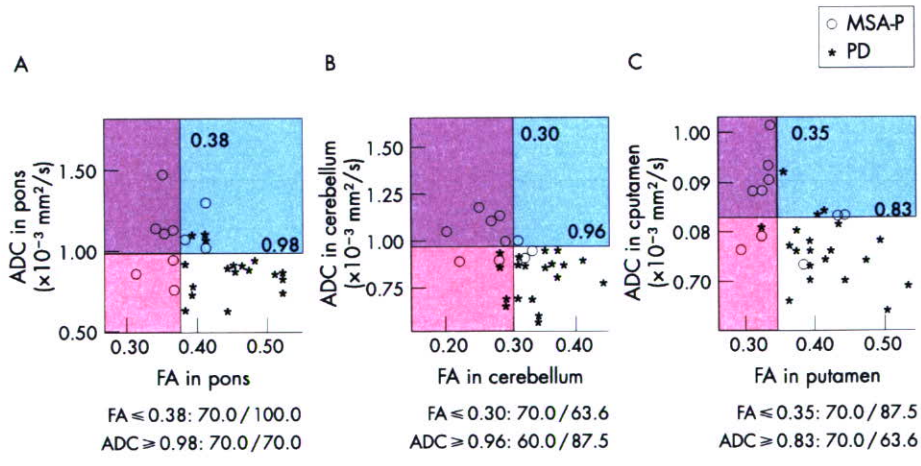

Figure 5 Differentiation of multiple system atrophy if parkinsonian features predominate (MSA-P) from Parkinson's disease (PD). Fractional anisotropy (FA) and apparent diffusion coefficient (ADC) values in the pons (A), cerebellum (B) and putamen (C). In the pons, cerebellum and putamen, the cut off point was set at 0.38, 0.30 and 0.35 for FA, and 0.98, 0.96 and 0.83 for ADC, respectively. Sensitivity/specificity in differentiating probable MSA-P from PD using these cut off points are shown. FA values in the pons were particularly useful for readily differentiating MSA-P from PD. In addition, some MSA-P cases had low FA and normal ADC values or normal FA and high ADC values. All patients that had both low FA and high ADC values in all three areas were MSA cases, and all patients that had both normal FA and ADC values in the pons were PD cases.

procedure to detect early involvement in MSA without diagnostic MRI findings. In particular, 90.0% of probable MSA-P cases showed a combination of low FA and high ADC values in one or more of the three areas, but no PD patients showed both low FA and high ADC values in any of the three areas. In addition, 57.1% of PD cases showed a combination of normal FA and ADC values in all three areas. These results suggest that combined evaluation of FA and ADC values in early disease stages provides an accurate method for differentiating MSA-P from PD.

ADC values measure the average water diffusion. High putaminal ADC values were reported to be helpful in differentiating MSA-P from PD.[12] Subsequently, brainstem ADC values in MSA-C were demonstrated to be increased.[13] As increases in ADC values have been shown in certain other diseases[19–21] and in normal aging,[22] high ADC values are thought to reflect destruction of tissue architecture. In contrast, FA values are new parameters specifically measuring the degree of anisotropy of the diffusing water along different axes of the image, enabling useful quantitative estimation of decreased tissue anisotropy reflecting degeneration. Reduced FA values have been reported in certain other diseases[23–25] and in normal aging.[26] More recently, decreased FA values in cerebellopetal fibres and pyramidal tracts have been reported in MSA-C,[14] and low FA values are also thought to reflect destruction of tissue architecture. In this study, we demonstrated that by using small voxels and optimised parameters,[16] as well as a generalised autocalibrating partially parallel acquisitions (GRAPPA)[17] algorithm for suppressing artefact and noise to obtain reliable ADC and FA values, as evidenced by clear tractography results, increased ADC and decreased FA values could reflect destruction of brainstem, cerebellar or putaminal tissue architecture resulting from neuronal loss and/or gliosis, enhancing random mobility of free water molecules within the tissue. Our results support previous observations and extend the significance of FA and ADC values in the diagnosis of MSA-P, even in cases without DPH or HCB signs.

Some of our MSA-P or PD cases showed a combination of normal FA but high ADC or low FA but normal ADC values in various regions. As above, high ADC and low FA values could reflect similar destruction of tissue architecture and have been demonstrated in various pathological changes, including brain atrophy, atherosclerotic change and normal aging.[22 26] However, these parameters are based on different pathological conditions. This may be one of the reasons why some cases showed normal FA but high ADC or low FA but normal ADC values. Furthermore, only cases of MSA-P had both low FA and high ADC values in each of the three areas. FA and ADC values may mutually provide additional information about the evolution of the disease that is not available from one method. These findings suggest that the combined evaluation of FA and ADC values could be more useful for early detection of pathological involvement in MSA-P than evaluation of either of these separately.

With respect to location, pontine FA and ADC values were especially useful markers in diagnosing MSA-P compared with those in the cerebellum and putamen. Although degeneration of olivopontocerebellar systems is evident from clinical features and MRI findings in MSA-C, these changes are not apparent in the early phase of MSA-P. The present study clearly demonstrated that even though reductions in FA values and increases in ADC values in the pons and cerebellum were more remarkable in MSA-C than in MSA-P, these changes were still highly evident in MSA-P. The question arises as to why significantly abnormal ADC and FA values can be seen in the pons even in early phase MSA. Patients with early stage MSA in Caucasian populations have been reported to show selective neuronal cell loss in the substantia nigra and locus coeruleus, with relative sparing of both the striatum and the olivopontocerebellar system.[27] One possible explanation may be that ADC and FA values have the potential to detect minimal and subclinical, but accumulated, neurodegeneration in the pons, because the pons contains the neurons and fibre tracts (eg, the pontine nuclei, transverse pontine fibres and corticospinal tracts) that are preferentially effected in MSA and thus could accumulate and reflect the MSA specific neurodegenerative process at an early phase of illness. Alternatively, it could be due to differences in the pathological features of MSA among Japanese and Caucasian populations. We previously reported that MSA-C was more frequent, and MSA-P less frequent, in Japanese populations[11] compared with Western populations,[3] and also that proton magnetic resonance spectroscopy (^{1}H-MRS) showed significantly lower N-acethylaspartate/creatine ratios in the basis pontis suggesting more neuroaxonal loss or dysfunction in MSA-P than in PD.[28] The olivopontocerebellar system shows more profound degeneration in Japanese MSA-P. While further study is needed to address this issue, we suggest that the pons is a beneficial region to detect early pathological change in MSA.

In previous reports,[12] ADC values in the dorsolateral putaminal ROIs were reported to be more useful in distinguishing MSA from PD compared with those in the anteroventral ROIs. It is interesting that this result corresponded well to the spatial distribution of pathological lesions in the putamen in MSA. In contrast, we used relatively large sized ROIs than previous reports to obtain reliable data under our MRI conditions, such as higher magnetic field strength, special software and parameters to analyse FA and ADC values. In addition, as some MSA and PD patients showed obscure putaminal edges on MRI, we set the ROIs in the relatively midst putamen, including dorsolateral parts. These specific MRI conditions may have caused the differences in the sensitivity and specificity in the putamen between our study and previous ones. These discrepancies may also be explained by ethnic differences. The olivopontocerebellar system could be more severely affected in Japanese than in Western populations. A multicentre survey will be needed to clarify the optimised size of ROIs, magnetic field strengths and parameters to standardise the FA and ADC values as diagnostic criteria.

In summary, combined evaluation of FA and ADC values in the putamen, cerebellum and putamen would provide useful information for highly and accurate differentiation of MSA-P from PD. Such early FA reduction and ADC increase are likely to be associated with subtle early degenerative processes in MSA, even without diagnostic magnetic resonance signal abnormalities. In addition, to justify our conclusion, it will be necessary to apply this algorithm, in a prospective manner, to patients with possible MSA without diagnostic MRI findings, and to determine whether these patients will develop full blown MSA symptoms in several years.

Authors' affiliations
Mizuki Ito, Hirohisa Watanabe, Yoshinari Kawai, Naoki Atsuta, Fumiaki Tanaka, Gen Sobue, Department of Neurology, Nagoya University Graduate School of Medicine, Nagoya, Japan
Shinji Naganawa, Hiroshi Fukatsu, Department of Radiology, Nagoya University Graduate School of Medicine, Nagoya, Japan

Competing interests: None.

REFERENCES

1 **Graham JG,** Oppenheimer DR. Orthostatic hypotension and nicotine sensitivity in a case of multiple system atrophy. *J Neurol Neurosurg Psychiatry* 1969;**32**:28–34.

2 **Quinn N.** Multiple system atrophy—the nature of the beast. *J Neurol Neurosurg Psychiatry* 1989;**52**:78–89.
3 **Wenning GK**, Tison F, Ben-Shlomo Y, *et al.* Multiple system atrophy: a review of 203 pathologically proven cases. *Mov Disord* 1997;**12**:133–47.
4 **Wenning GK**, Colosimo C, Geser F, *et al.* Multiple system atrophy. *Lancet Neurol* 2004;**3**:93–103.
5 **Gilman S**, Low PA, Quinn N, *et al.* Consensus statement on the diagnosis of multiple system atrophy. *J Neurol Sci* 1999;**163**:94–8.
6 **Wenning GK**, Ben-Shlomo Y, Hughes A, *et al.* What clinical features are most useful to distinguish definite multiple system atrophy from Parkinson's disease? *J Neurol Neurosurg Psychiatry* 2000;**68**:434–40.
7 **Savoiardo M**, Strada L, Girotti F, *et al.* Olivopontocerebellar atrophy: MR diagnosis and relationship to multiple system atrophy. *Radiology* 1990;**174**:693–6.
8 **Konagaya M**, Konagaya Y, Iida M. Clinical and magnetic resonance imaging study of extrapyramidal symptoms in multiple system atrophy. *J Neurol Neurosurg Psychiatry* 1994;**57**:1528–31.
9 **Schrag A**, Kingsley D, Phatouros C, *et al.* Clinical usefulness of magnetic resonance imaging in multiple system atrophy. *J Neurol Neurosurg Psychiatry* 1998;**65**:65–71.
10 **Kraft E**, Schwarz J, Trenkwalder C, *et al.* The combination of hypointense and hyperintense signal changes on T2-weighted magnetic resonance imaging sequences: a specific marker of multiple system atrophy? *Arch Neurol* 1999;**56**:225–8.
11 **Watanabe H**, Saito Y, Terao S, *et al.* Progression and prognosis in multiple system atrophy: an analysis of 230 Japanese patients. *Brain* 2002;**125**:1070–83.
12 **Schocke MF**, Seppi K, Esterhammer R, *et al.* Trace of diffusion tensor differentiates the Parkinson variant of multiple system atrophy and Parkinson's disease. *Neuroimage* 2004;**21**:1443–51.
13 **Kanazawa M**, Shimohata T, Terajima K, *et al.* Quantitative evaluation of brainstem involvement in mutiple system atrophy by diffusion-weighted MR imaging. *J Neurol* 2004;**251**:1121–4.
14 **Shiga K**, Yamada K, Yoshikawa K, *et al.* Local tissue anisotropy decreases in cerebellopetal fibers and pyramidal tract in multiple system atrophy. *J Neurol* 2005;**252**:589–96.
15 **Calne DB**, Snow BJ, Lee C. Criteria for diagnosing Parkinson's disease. *Ann Neurol* 1992;**32**:S125–7.
16 **Naganawa S**, Koshikawa T, Kawai H, *et al.* Optimization of diffusion-tensor MR imaging data acquisition parameters for brain fiber tracking using parallel imaging at 3T. *Eur Radiol* 2004;**14**:234–8.
17 **Griswold MA**, Jakob PM, Heidemann RM, *et al.* Generalized autocalibrating partially parallel acquisitions (GRAPPA). *Magn Reson Med* 2002;**47**:1202–10.
18 **Bhattacharya K**, Saadia D, Eisenkraft B, *et al.* Brain magnetic resonance imaging in multiple-system atrophy and Parkinson disease. *Arch Neurol* 2002;**59**:835–42.
19 **Schaefer PW**, Grant PE, Gonzalez RG. Diffusion-weighted MR imaging of the brain. *Radiology* 2000;**217**:331–45.
20 **Wilson M**, Morgan PS, Lin X, *et al.* Quantitative diffusion weighted magnetic resonance imaging, cerebral atrophy, and disability in multiple sclerosis. *J Neurol Neurosurg Psychiatry* 2001;**70**:318–22.
21 **Kantarci K**, Jack CR, Xu YC, *et al.* Mild cognitive impairment and Alzheimer disease: Regional diffusivity of water. *Radiology* 2001;**219**:101–7.
22 **Helenius J**, Soinne L, Perkio J, *et al.* Diffusion-weighted MR imaging in normal human brains in various age groups. *Am J Neuroradiol* 2002;**23**:194–9.
23 **Toosy AT**, Werring DJ, Orrell RW, *et al.* Diffusion tensor imaging detects corticospinal tract involvement at multiple levels in amyotrophic lateral sclerosis. *J Neurol Neurosurg Psychiatry* 2003;**74**:1250–7.
24 **Sugihara S**, Kinoshita T, Matsusue E, *et al.* Usefulness of diffusion tensor imaging of white matter in Alzheimer disease and vascular dementia. *Acta Radiol* 2004;**45**:658–63.
25 **Guo AC**, MacFall JR, Provenzale JM. Multiple sclerosis: diffusion tensor MR imaging for evaluation of normal appearing white matter. *Radiology* 2002;**222**:729–36.
26 **Abe O**, Aoki S, Hayashi N, *et al.* Normal aging in the central nervous system: quantitative MR diffusion-tensor analysis. *Neurobiol Aging* 2002;**23**:433–41.
27 **Wenning GK**, Quinn N, Magalhaes M, *et al.* "Minimal change" multiple system atrophy. *Mov Disord* 1994;**9**:161–6.
28 **Watanabe H**, Fukatsu H, Katsuno M, *et al.* Multiple regional 1H-MR spectroscopy in multiple system atrophy: NAA/Cr reduction in pontine base as a valuable diagnostic marker. *J Neurol Neurosurg Psychiatry* 2004;**75**:103–9.

nature medicine

ASC-J9 ameliorates spinal and bulbar muscular atrophy phenotype via degradation of androgen receptor

Zhiming Yang[1,2,7], Yu-Jia Chang[1,3,7], I-Chen Yu[1], Shuyuan Yeh[1], Cheng-Chia Wu[1,3], Hiroshi Miyamoto[1], Diane E Merry[4], Gen Sobue[5], Lu-Min Chen[1,6], Shu-Shi Chang[1,6] & Chawnshang Chang[1]

Motor neuron degeneration resulting from the aggregation of the androgen receptor with an expanded polyglutamine tract (AR-polyQ) has been linked to the development of spinal and bulbar muscular atrophy (SBMA or Kennedy disease). Here we report that adding 5-hydroxy-1,7-bis(3,4-dimethoxyphenyl)-1,4,6-heptatrien-3-one (ASC-J9) disrupts the interaction between AR and its coregulators, and also increases cell survival by decreasing AR-polyQ nuclear aggregation and increasing AR-polyQ degradation in cultured cells. Intraperitoneal injection of ASC-J9 into AR-polyQ transgenic SBMA mice markedly improved disease symptoms, as seen by a reduction in muscular atrophy. Notably, unlike previous approaches in which surgical or chemical castration was used to reduce SBMA symptoms, ASC-J9 treatment ameliorated SBMA symptoms by decreasing AR-97Q aggregation and increasing VEGF164 expression with little change of serum testosterone. Moreover, mice treated with ASC-J9 retained normal sexual function and fertility. Collectively, our results point to a better therapeutic and preventative approach to treating SBMA, by disrupting the interaction between AR and AR coregulators.

X-linked spinal and bulbar muscular atrophy (SBMA or Kennedy disease) is an inherited neurodegenerative disorder caused by the expansion of the polyglutamine tract of the androgen receptor (AR-polyQ)[1–3]. The length of the AR-polyQ tract is inversely correlated with the age of SBMA onset[1–3]. The effects of the disease are only seen in males, as female carriers are usually asymptomatic. Characteristics of SBMA include proximal muscular atrophy, weakness, contraction fasciculation and bulbar involvement[4]. The nuclear inclusions containing AR-polyQ in the residual motor neurons of the brain stem, spinal cord and other visceral organs[5] are considered to be relevant to the pathophysiology of this disease[6].

In normal individuals, AR (ref. 7), upon activation by androgen, functions as a transcriptional regulator[8] by interacting with a variety of coregulatory proteins[9,10]. In motor neurons, one of the key AR coregulators is the cAMP response element–binding protein (CREB)-binding protein (CBP)[11], which controls the expression of the gene encoding VEGF164 among other genes.

Several mechanisms have been proposed to explain the pathogenesis of SBMA and to suggest potential targets for medical intervention. These mechanisms, which are not necessarily mutually exclusive, include transcriptional deregulation[12], aggregate formation[11,13], proteolysis of causative proteins[14,15], transglutaminase activation[16] and mitochondrial deficits[17]. Transcriptional disturbance, for example through the sequestration of CBP by AR-polyQ aggregates, seems to be one of the most likely causes for the pathogenesis of SBMA. This notion is further supported by the fact that transcriptional deregulation occurs in polyQ-related diseases[18]. Consistent with this idea, manipulations such as chemical or surgical castration, which reduce the level of AR-97Q aggregates[19–21], as well as the administration of a histone deacetylase inhibitor, which restores CBP-mediated transcription, effectively treat SBMA in mice[20]. However, the severe side effects caused by castration, including loss of libido, impotence, osteoporosis and fatigue, and the toxicity of histone deacetylase inhibitors make these approaches unsuitable therapeutic strategies for treating SBMA in men.

A compound that disrupts aggregates comprised of AR-polyQ and various coregulators could have potential therapeutic benefits for two complementary reasons. First, such a compound could increase the level of transcriptionally active coregulators, including CBP, by releasing them from the nonproductive interaction with AR-polyQ. Second, disrupting the aggregates might render the released AR-polyQ more vulnerable to degradation, thereby reducing its toxic effect.

We screened natural products and their derivatives for the disruption of normal AR and its coregulators, and found that 5–hydroxy-1,7-bis(3,4-dimethoxyphenyl)-1,4,6-heptatrien-3-one (ASC-J9) can substantially promote the dissociation of AR and ARA70 (ref. 22). Moreover, we discovered that treatment of prostate cancer cells with ASC-J9 led to decreased AR transactivation, resulting in the suppression of AR-mediated cell proliferation[22]. Using a SBMA PC12/AR-112Q cell line[23] and a SBMA/AR-97Q line of transgenic mice[5] as models, we found that ASC-J9 ameliorated SBMA symptoms with little influence on the concentration of circulating testosterone.

[1]George Whipple Lab for Cancer Research, Departments of Pathology, Urology, and Radiation Oncology, and The Cancer Center, University of Rochester Medical Center, Rochester, New York 14642, USA. [2]Zhejiang University and 2nd Hospital, Hangzhou 310009, China. [3]Taipei Medical University and Hospital, Taipei 110, Taiwan. [4]Thomas Jefferson University, Philadelphia, Pennsylvania 19107, USA. [5]Nagoya University, Nagoya 466-8550, Japan. [6]China Medical University and Hospital, Taichung 404, Taiwan. [7]These authors contributed equally to this work. Correspondence should be addressed to C.C. (chang@URMC.rochester.edu).

Received 10 March 2006; accepted 16 January 2007; published online 4 March 2007; doi:10.1038/nm1547